

We are IntechOpen, the world's leading publisher of Open Access books Built by scientists, for scientists

4,800

Open access books available

122,000

International authors and editors

135M

Downloads

Our authors are among the

154

Countries delivered to

TOP 1%

most cited scientists

12.2%

Contributors from top 500 universities



WEB OF SCIENCE™

Selection of our books indexed in the Book Citation Index
in Web of Science™ Core Collection (BKCI)

Interested in publishing with us?
Contact book.department@intechopen.com

Numbers displayed above are based on latest data collected.
For more information visit www.intechopen.com



Scanning Probe Lithography on Organic Monolayers

SunHyung Lee¹, Takahiro Ishizaki², Katsuya Teshima¹,
Nagahiro Saito³ and Osamu Takai³

¹*Faculty of Engineering, Shinshu University,*

²*National Institute of Advanced Industrial Science and Technology (AIST),*

³*EcoTopia Science Institute, Nagoya University,*

Japan

1. Introduction

Lithographic technologies for the surface modification of inorganic and organic surfaces have been developed for various devices such as sensing, data memory, single molecule electronics and biological systems. Nano and micropatterning of organic monolayers have attracted attentions for applications to biological systems in which proteins or DNA are fixed. Photolithography, microcontact printing, and electron beam lithography have usually been used as patterning techniques for organic monolayers (Hayashi et al., 2002; Hong et al., 2003; Saito et al., 2003; Hahn et al., 2004; Kidoaki & Matsuda, 1999). Although the electron-beam lithography can fabricate very small patterns, it requires an ultra-high vacuum system (Harnett et al., 2001). The resolution of photolithography is limited by the light wavelength. Moreover, these methods are based on destructive lithography, i.e., they cause damages to the organic materials.

In particular, nano-lithographic technologies have evolved in order to satisfy persistent demands for miniaturization and high-density integration of semiconductor electric circuits. Scanning probe microscopy (SPM) has been a key tool in achieving this goal. SPM can be used not only as the means that observe surface structure at sub-molecule level by a probe but also as the means that control the atomic and molecular arrangement on a substrate. As a local nano-fabrication means, the lithography technique in nanoscale range by using SPM is called to the scanning probe lithography (SPL) (Kaholek et al., 2004; Blackledge et al., 2000; Tello et al., 2002; Liu et al., 2002). In particular, a variety of lithographic techniques using SPM probe can fabricate nano-scale patterns on an organic monolayer, such as nanoshaving, nanografting, anodization SPL, dip-pen nanolithography (DPN), and electrochemical SPL. The lithography technique is used to break the material surface by using various energy sources. SPM can also be used to break the organic monolayer. For instance, nanoshaving involves mechanical scratching by physical pressure of the probe, and anodization lithography involves anodic oxidation of the substrate surface by an applied bias voltage (above 9 V) between the probe and the substrate (Jang et al., 2002; Kaholek et al., 2004; Sugimura, & Nakagiri, 1995). In the case of the anodization lithography, the oxide layer can be fabricated by anodic oxidation. As another SPL technique, the

nanografting procedure combines the fabrication of a nanopattern and the binary SAM using atomic force microscopy (AFM) (Amro et al., 2000; Xu et al., 1999; Liu et al., 2000). As the other process, a probe is scanned on the matrix SAM at a high force. The matrix SAM is removed and simultaneously replaced by another molecule in the scanning area. Fig. 1 shows the nanoshaving, nanografting, and anodization lithography techniques.

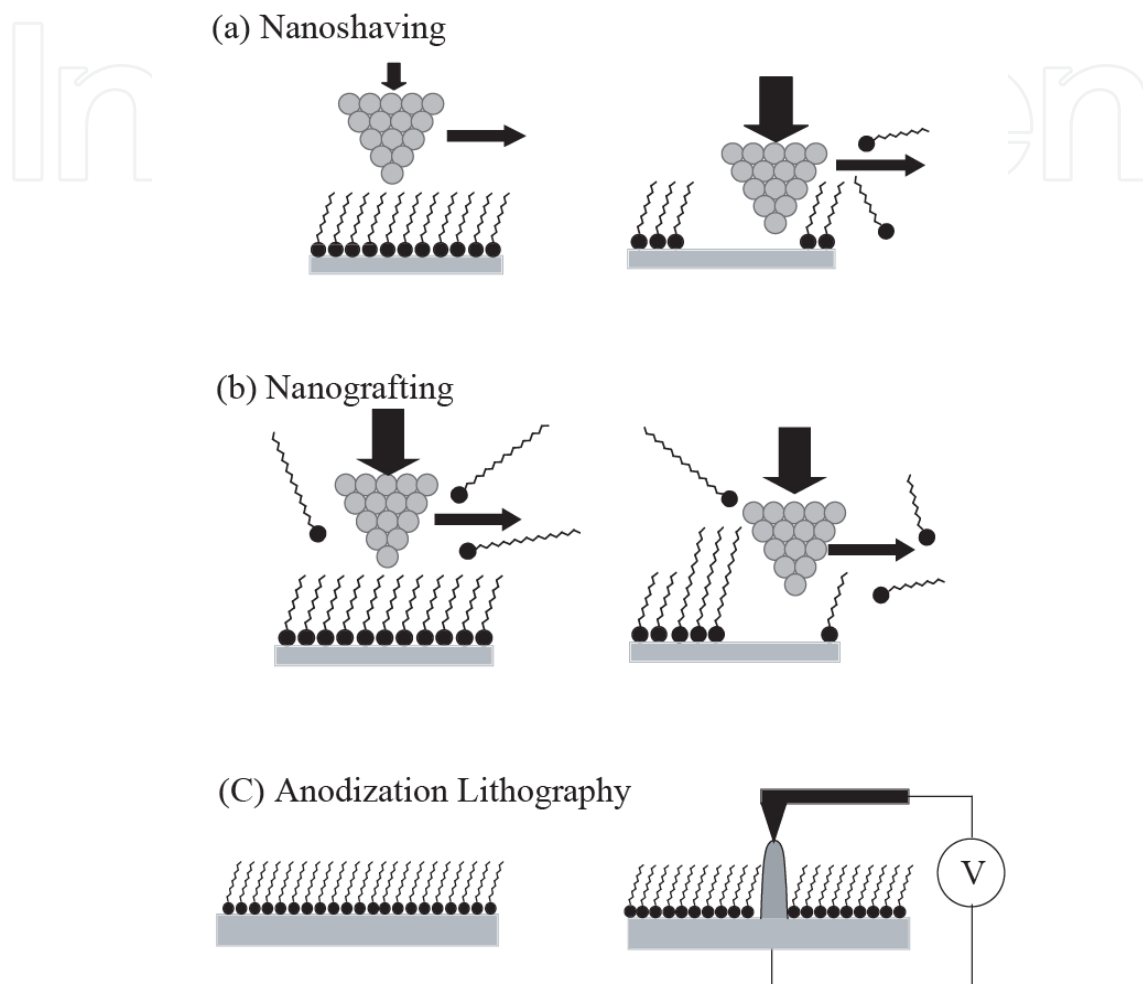


Fig. 1. Various lithographic methods using SPM probe on the organic monolayer. : (a) nanoshaving, (b) nanografting and (c) anodization lithography

In addition, dip-pen nanolithography (DPN) is a nanopatterning technique with a probe which delivers molecules to a surface via a water meniscus in the ambient atmosphere (Pena et al., 2003; Schwartz, 2002; Maynor. et al., 2004). This direct-writing technique offers high-resolution patterning capabilities for a number of molecular and biomolecular materials (ink) on a variety of substrates (paper). Nanografting and DPN are recently developed as “soft” lithographic methods, which do not cause any damage to the organic monolayers. Electrochemical SPL is also one of the soft lithographic methods. This is performed through the water column condensed between the tip of the SPM and the substrate surface. This water column can be used as a minute electrochemical cell. When a bias voltage is applied, a redox reaction occurs on the substrate surface. In the case of SAM, the functional group is converted by this redox reaction and a nanopattern is formed on the SAM surface. Fig. 2 shows the DPN and electrochemical SPL techniques.

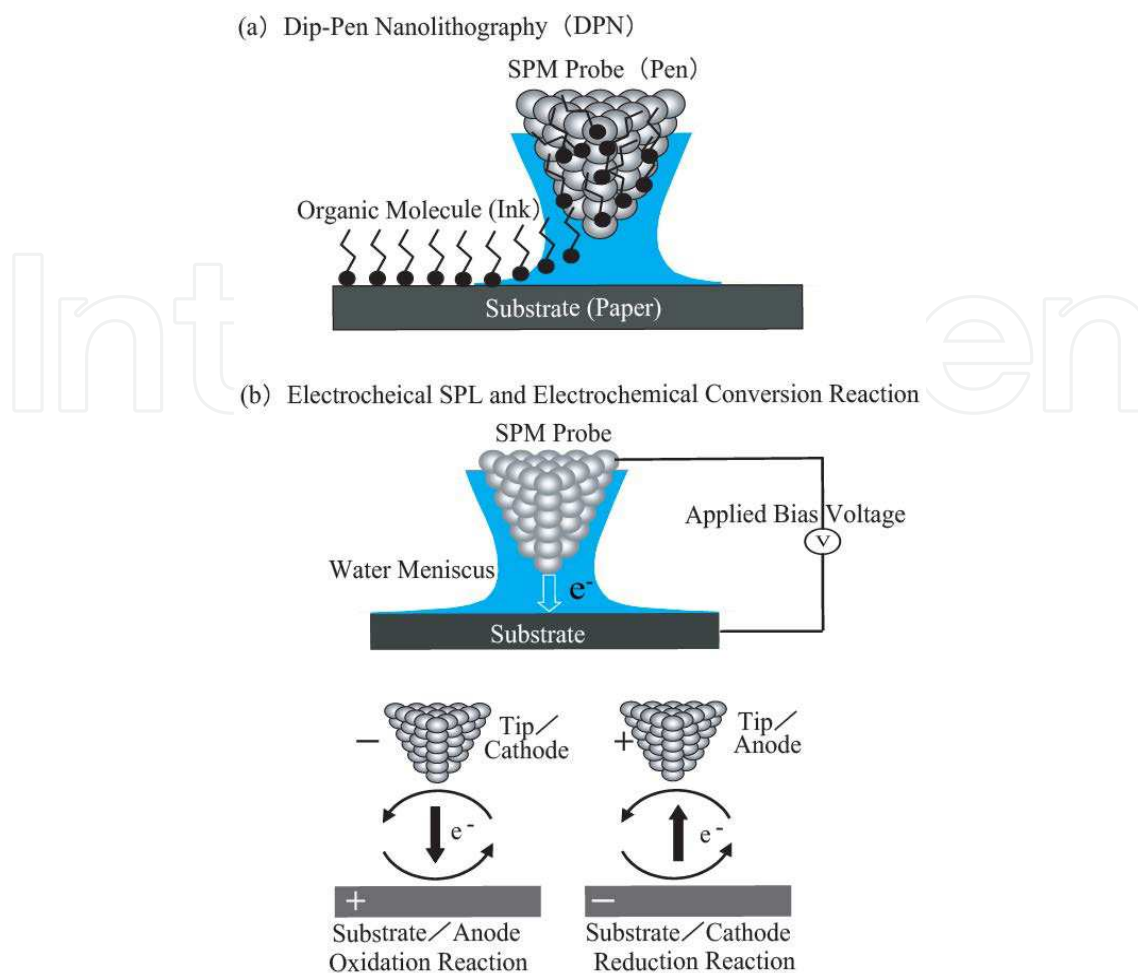
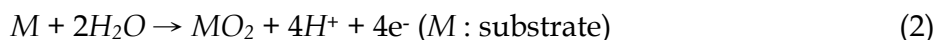


Fig. 2. Schematic illustration of dip-pen nanolithography (DPN) and electrochemical SPL.

In this chapter, we introduce anodization SPL and electrochemical SPL for fabricating the nanostucture and controlling the function group on the various organic monolayers, such as organosilane self-assembled monolayers (SAMs) and the monolayer covalently attached to silicon through Si-C bond. First, anodization SPL techniques are expected to fabricate nanostructures on surfaces of electronic device. Their technique can remove an organic monolayer and fabricate an oxide structure by applying highly bias voltage between probe and substrate. When a high positive bias voltage is applied to the probe, an oxidation reaction proceeds and an oxide structure forms on the surface. The electrochemical reactions on SPM probe and substrate are shown in Eqs., respectively (Lee et al., 2009).



In these reactions, electric characteristics of coated materials on the probes are important to formation of an oxide structure. The oxide structure is easily fabricated on the substrate by anodization SPL since the silicon oxide insulator layer is removed. However, the oxide structure is difficult to control and is not attained to single nanometer level though many researchers have reported on anodization SPL. We introduced fabricating technique of a three-dimensional nanostructure (nanoline structure) of silicon oxide on the hydrogen-

terminated Si substrates by anodization SPL, and the effects of coated materials of SPM probe on the sizes of oxidized structures (Lee et al., 2009).

Second, we introduce a novel soft lithography based on electrochemistry through scanning probe electrochemistry for controlling the functional group on the organic monolayers (Lee et al., 2007; Lee & Ishizaki et al., 2007; Saito et al., 2005; Sugimura et al., 2004). Scanning probe electrochemistry in which materials surfaces locally oxidized or reduced by a tip of SPM is a promising technique for constructing nanostructures consisting of organic molecules. This electrochemical SPL is performed through water column which is condensed between the tip of SPM and the substrate surface. This water column can be used as a microscopic electrochemical cell. In the case of electrochemical conversion using a nanoprobe, the electrochemical reactions which proceed at the probe-sample junction are governed by the applied bias voltage and its polarity. When the substrate is polarized positively, anodic reactions, that is, oxidation reactions, proceed on its surface. On the contrary, when the substrate is polarized negatively, cathodic reactions, that is, reductive reactions, proceed. The method is expected as a key technology for future molecular nanodevices. In addition, organosilane self-assembled monolayers (SAMs) have been applied to a resist material for SPL. Here we report the chemical conversion of an organic molecular monolayer in a reversible manner using SPM. The chemical state of the monolayer from its oxidized state to reduced state or vice versa is controlled. First, an amino-terminated SAM was chemically converted into an oxidized SAM by SPL at positive-bias voltages. Moreover, this oxidized SAM was then reconverted into an amino-terminated SAM by SPL at negative bias voltages. We examine the chemical changes undergone in the scanned area from the viewpoint of surface-potential reversibility. Additionally, we introduce a electrochemical SPL to fabricate -COOH groups on an organic monolayer directly attached to silicon, which was synthesized from 1,7-octadien (OD) and hydrogen-terminated silicon. The -COOH groups on the OD-monolayer were also synthesized by the properties of surface produced by SPL.

2. Anodization scanning probe lithography on the organic monolayer on the hydrogen-terminated Si substrate

In this chapter, we introduced fabricating technique of a three-dimensional nanostructure of organic monolayer on the hydrogen-terminated Si substrates by anodization SPL. First, we fabricated the organic monolayer on the hydrogen-terminated Si(111) wafers with an electrical resistance of 10.0-20.0 Ω -cm. Si substrates were sonicated in acetone and ethanol for 10 min, and then, cleaned by an ultraviolet (UV) light/ozone cleaning method. The substrates were exposed to vacuum UV (VUV) light (172 nm) from an excimer lamp for 30 min under atmospheric pressure and room temperature. Subsequently, the substrates were cleaned in piranha solution ($\text{H}_2\text{SO}_4:\text{H}_2\text{O}_2 = 3:1$) at 100 °C for 10 min and rinsed in ultrapure water. They were then etched for 15 min by immersing in 40 % aqueous ammonium fluoride solution (NH_4F). As a result, the native silicon oxide layer was removed from the substrates, and hydrogen-terminated surfaces were formed. 1-decane monolayer was prepared by a liquid phase method. The hydrogen-terminated substrates were immersed in the solution of 1-decane molecules at 150 °C for 3 h. After the immersion, the organic monolayer coated substrates were cleaned in toluene, acetone, and ethanol, and rinsed in ultrapure water. Firstly, the 1-decane monolayer was fabricated on the hydrogen-terminated Si substrates through a liquid phase method at 150 °C. Fig. 3(a) shows the chemical structure of 1-decane

molecule. The static water contact angle and film thickness of the monolayer was about 107° and 1.12 nm, respectively. A smooth surface coated with densely packed CH_3 groups (alkyl monolayer) shows a water contact angle of approximately 110° . In addition, its thickness was considered reasonable since the chain length of 1-decane molecule was estimated to be 1.32 nm. It is indicated that the 1-decane molecules formed an organic monolayer on the silicon substrate. Fig. 3(b) shows the XPS Si2p spectrum of the Si surface coated with the 1-decane monolayer. As clearly shown in Fig. 3(b), the peak of native silicon oxide was not observed at all. These results indicate that the 1-decane molecules reacted directly to the hydrogen-terminated silicon surfaces and formed the organic monolayer there. Fig. 3(c) and 3(d) show the AFM topographic and friction images of the Si surfaces after immersing in 1-decane solution. The flat terraces with steps for silicon one-atom and the changes of high friction on steps were, respectively, observed on the topographic and friction images. In the topographic image [Fig. 3(c)], the intervals of the steps and the terraces were 180 nm and $3.2 \pm 0.3 \text{ \AA}$, respectively. In addition, the difference of friction force between the flat terraces and steps was about 10 mV. These results indicated to the surface profiles of hydrogen-terminated silicon. It was therefore found that the 1-decane molecules were vertically and densely assembled, and their monolayer was formed through doubly-bonded terminated group attached to the hydrogen-terminated silicon surface.

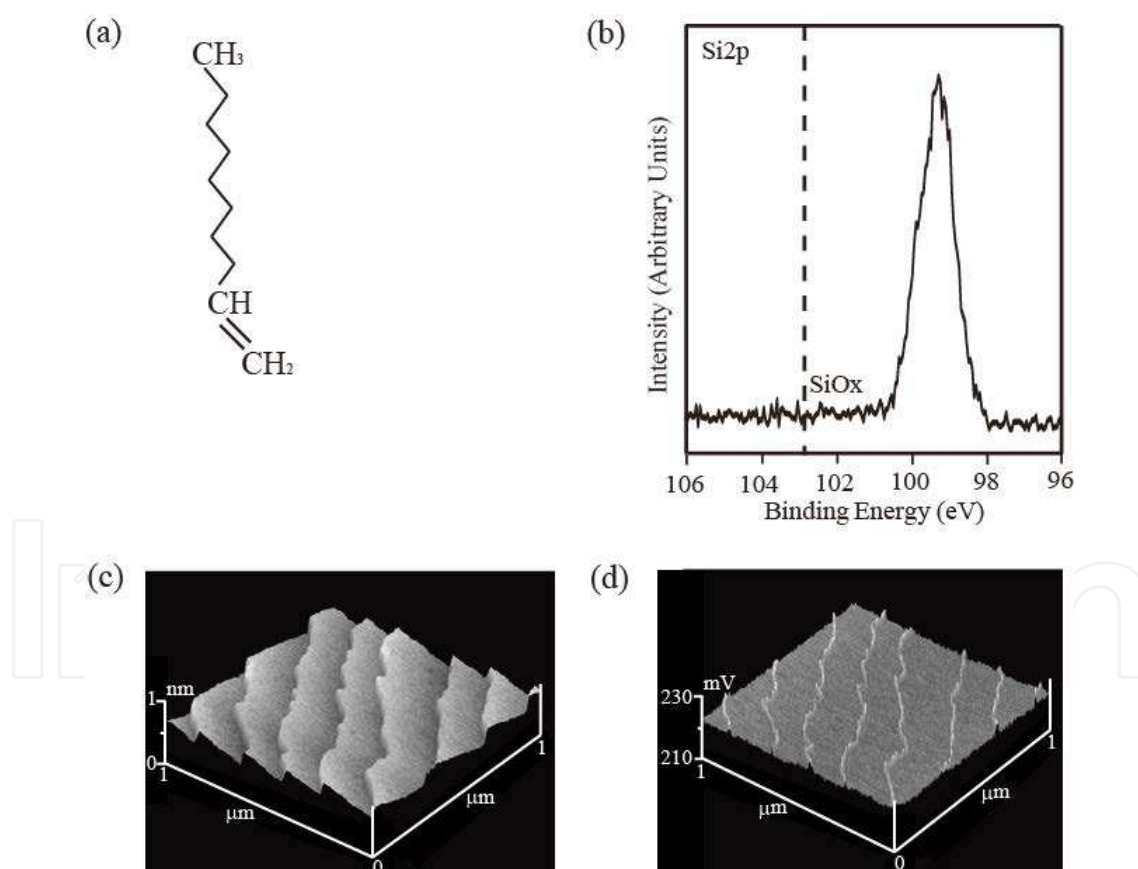


Fig. 3. (a) The chemical structure of 1-decane (b) XPS Si2p spectra (c) topographic image (d) friction image of sample surfaces after prepared 1-decane monolayer. [SH. Lee, N. Saito, O. Takai, Highly reproducible technique for three-dimensional nanostructure fabrication via anodization scanning probe lithography, *Appl. Surf. Sci.*, 255, 7302-7306 (2009). Copyright@ELSEVIER (2009)]

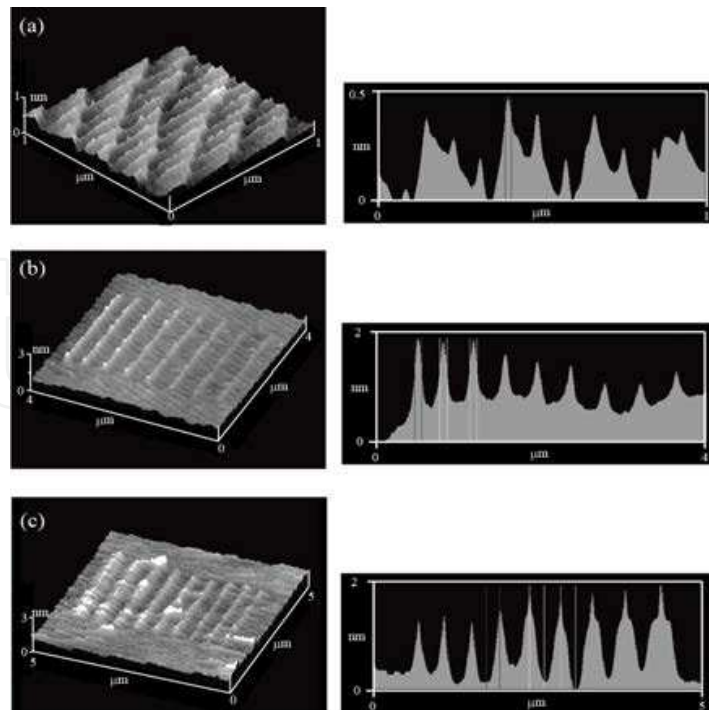


Fig. 4. The topographic images of SiO_x line structure fabricated on the 1-decane monolayer and profiles for each topographic image by using various tip: (a) diamond coated Si tip, (b) Si tip and (c) Au coated Si tip. [SH. Lee, N. Saito, O. Takai, Highly reproducible technique for three-dimensional nanostructure fabrication via anodization scanning probe lithography, *Appl. Surf. Sci.*, 255, 7302-7306 (2009). Copyright@ELSEVIER (2009)]

Next, we investigated that the effect of scanning rate on nanoline width of silicon oxide fabricated by anodization SPL. An anodization SPL was carried out on the 1-decane monolayer in air (humidity in ranging from 30 to 40 %) at the applied bias voltage of 9 V. In the anodization SPL, 1-decane monolayer was removed and the SiO_x nanoline structures were formed by scanning the probes. Fig. 4(a)-4(c) show the topographic images and profiles of SiO_x nanoline structure fabricated by the anodization SPL. In these experiments, various probes were used to fabricate oxide nanostructures [Fig. 4(a); diamond-coated Si probe, Fig. 4(b); Si probe (i.e., uncoated Si probe), Fig. 4(c); Au-coated Si probe]. Additionally, we investigated the effect of coated materials on the formation of the oxide nanostructure. The ranging of scanning rates for SPL is 0.1 to 5 μm/s. In these topographic images, the nanoline structure and flat terraces with steps were obviously observed under all scanning conditions. However, the widths of nanoline structures were changed with the scanning rates. Fig. 5 shows the variation in the width of nanoline structures with scanning rates and surface compositions of probes. When the diamond coated probe is used for anodization SPL, the nanoline widths were found to remain constant under all scanning conditions, and the scanning rates had no effect on the line width. The width was approximately 15 nm, which is one of the finest nanostructures in the field of SPL technique. The highly reproducible structure was fabricated by anodization SPL using the diamond-coated Si probe, and this technique is thought to be able to apply various industrial fields. On the other hand, when the Si probe (uncoated-Si) and Au-coated Si probe were used for anodization SPL, the line widths were markedly changed with the scanning rates. In the case of Au-coated Si probe, as the scanning rate increased from 0.1 to 5 μm/s, the width of

line structures drastically decreased from 375 to 125 nm. For Si probe (uncoated Si probe), the line width gradually decreased with increasing scanning rate, reaching about 100 nm at 5 $\mu\text{m}/\text{s}$. The width variations were Au-coated Si probe > Si probe (uncoated) > diamond-coated Si probe. These variations of the line width could be explained the band-gap energy of the coated materials. The band-gap energies of Au, Si and diamond are respectively about 0, 1.2 and 5.47 eV. That is to say, their conductive property is thought to be greatly dependent on the line width. These results indicate that high reproducibility of oxide nanoline structures is attainable by means of anodization SPL using the diamond-coated probe or a probe which has relatively low conductivity.

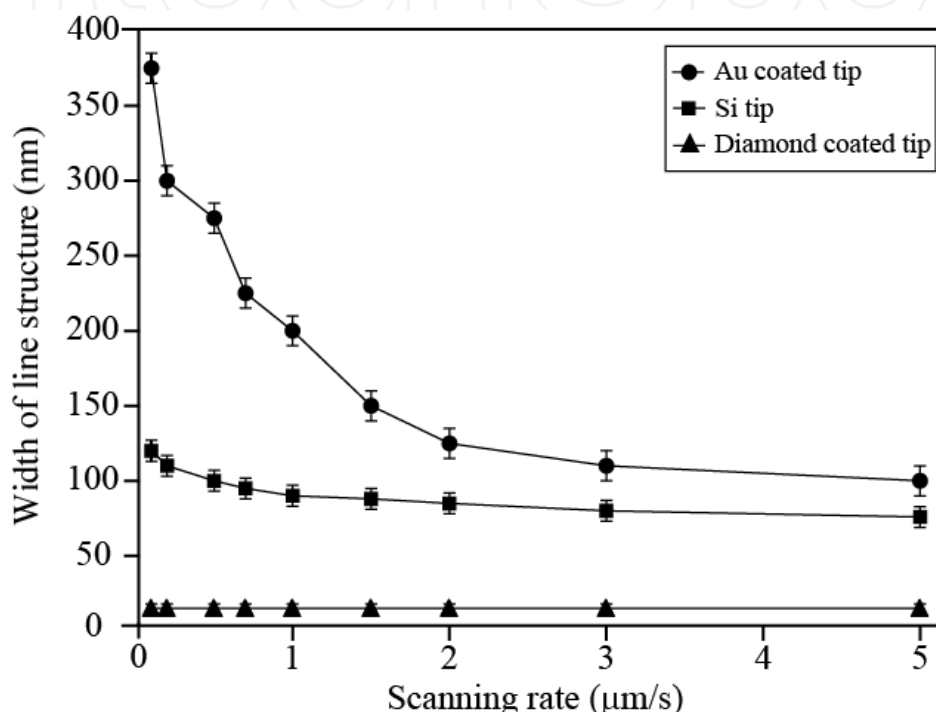


Fig. 5. The change of the line width with increasing scanning rate [SH. Lee, N. Saito, O. Takai, Highly reproducible technique for three-dimensional nanostructure fabrication via anodization scanning probe lithography, *Appl. Surf. Sci.*, 255, 7302-7306 (2009). Copyright@ELSEVIER (2009)]

Finally, the effect of applied bias voltage on nanoline width of silicon oxide was investigated by use of various SPM probes. Fig. 6(a)-(c) show the topographic images of SiO_x nanoline structures fabricated by diamond-coated Si, Si (uncoated) and Au-coated Si probes, respectively. The applied bias voltage and scanning rate were, respectively, fixed at 7 V and 1 $\mu\text{m}/\text{s}$. The obtained widths were 15, 60 and 100 nm in Fig. 6(a)-(c), respectively. The line width fabricated at the bias voltage of 7 V decreased compared to that at 9 V when Au-coated Si and uncoated Si probes were used. For the diamond-coated probe, the nanoline structure maintained the width of 15nm, that is, the applied bias voltages had no effect on the nanoline width. These results are also attributed to the band-gap energy of the coated materials. In particular, three-dimensional oxide nanostructures fabricated by the diamond-coated probe showed highly reproducibility even though various scanning rates and applied bias voltages are used in anodization SPL. Therefore, this technique is expectable to be applied to fabricate a wide variety of nanodevices, that have three-dimensional structures, in various industrial fields.

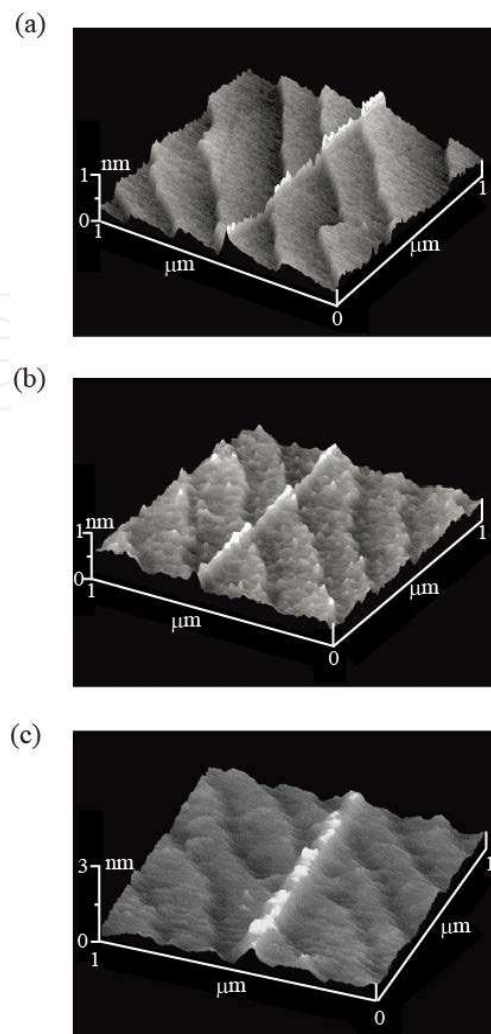


Fig. 6. Topographic images of line structure fabricated by (a) diamond coated Si tip, (b) Si tip and (c) Au coated Si tip, respectively. The applied bias voltage and scanning rate are 7 V and $1\mu\text{m/s}$, respectively. [SH. Lee, N. Saito, O. Takai, Highly reproducible technique for three-dimensional nanostructure fabrication via anodization scanning probe lithography, *Appl. Surf. Sci.*, 255, 7302-7306 (2009). Copyright@ELSEVIER (2009)]

3. Electrochemical scanning probe lithography on organic monolayer

A future tool of nanolithography may be nanopattern drawing based on SPM. Several reports describe SPL in which a sample surface is chemically converted or mechanically deformed at the probe-sample junction. The characteristic feature of all these methods is that they allow permanent nanopatterns to be drawn on the substrate. Scanning probe electrochemistry in which materials surfaces locally oxidized or reduced by a tip of SPM is a promising technique for constructing nanostructures consisting of organic molecules. This electrochemical SPL is performed through water column which is condensed between the tip of SPM and the substrate surface. This water column can be used as a microscopic electrochemical cell. When the bias voltage is applied, redox reaction proceeds on the substrate surface. The method is expected as a key technology for future molecular nanodevices. In addition, organosilane SAMs have been applied to a resist material for SPL.

4. Nano-probe electrochemistry on amino-terminated self-assembled monolayers toward nano memory

In this chapter, we investigated that an amino-terminated SAM was electrochemically converted into an oxidized SAM by SPL at positive bias voltages. Moreover, this oxidized SAM was then reconverted into an amino-terminated SAM by SPL at negative bias voltages. The chemical conversions of amino groups were confirmed by Kelvin probe force microscopy (KPFM), atomic force microscopy (AFM) and the site-selective adsorption of carboxyl-modified fluorescent spheres. We examined the chemical changes undergone in the scanned area from the viewpoint of surface-potential reversibility. Fig. 7 schematically illustrates of the experimental procedure. An amino-terminated SAM was prepared by chemical vapor deposition (CVD) from *p*-aminophenyltrimethoxysilane (APhS) on *n*-type silicon (111) wafers with electrical resistivity of 4-6 Ω /cm. First, the silicon substrate was cleaned in acetone, ethanol, and deionized water, in that order. After cleaning, the silicon substrate was irradiated by 172 nm vacuum ultraviolet light in air for 20 min. This removed organic contaminants and introduced silanol groups onto the substrate surface. Next, each cleaned silicon substrate was placed together with a glass vessel filled with APhS liquid in a Teflon container. The Teflon container was sealed and placed in an oven with the temperature kept at 100 °C. The reaction time was 1 h. The heated APhS liquid vaporized and hydrolyzed. The hydrolyzed APhS reacted with the silanol groups on the silicon substrate resulting in the fabrication of an amino-terminated SAM.

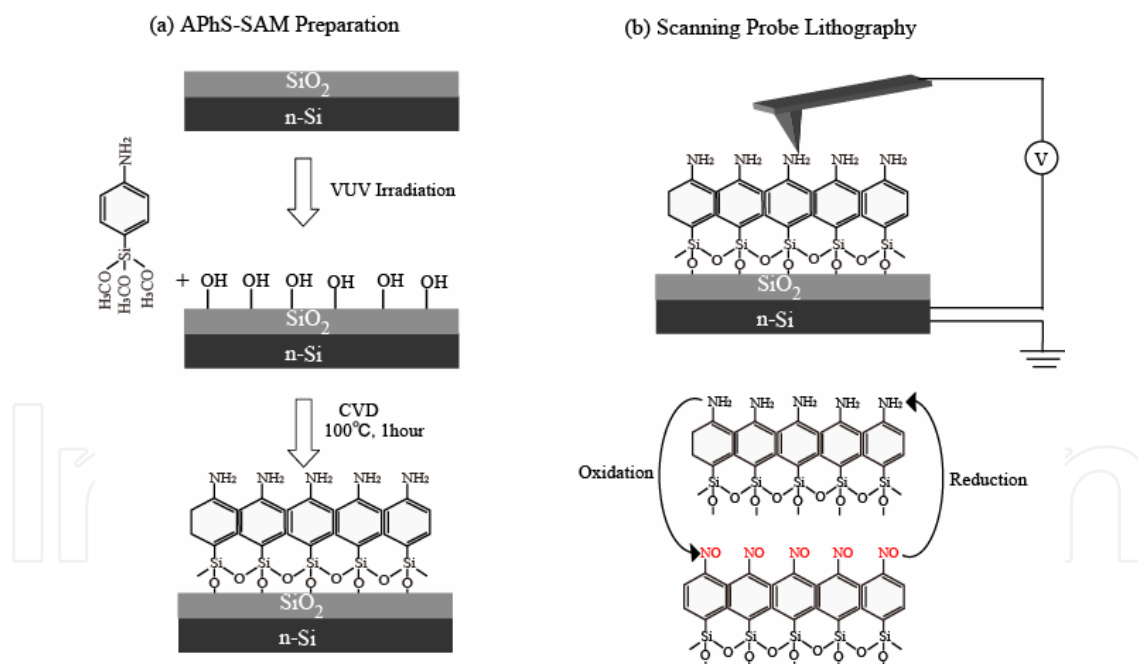


Fig. 7. Preparation and electrochemical scanning probe lithography of APhS-SAM [N. Saito, SH. Lee, T. Ishizaki, J. Hieda, H. Sugimura, O. Takai, Surface potential reversibility of an amino-terminated self-assembled monolayer based on nanoprobe chemistry, *J. Phys. Chem. B*, 109, 11602-11605 (2005) . Copyright@American Chemical Society (2005)]

We fabricated the APhS-SAM through the CVD method. The formation of APhS SAM was confirmed by the ellipsometry, water contact angle and X-ray photoelectron spectroscopy (XPS) measurement. In our SPL system, electrons were transferred between a gold-coated

probe and the silicon substrate through the APhS SAM and an adsorbed water layer. The adsorbed water played the same role as water in a typical, macroscopic electrochemical cell system. The electrochemical conversion was conducted with a gold-coated silicon nanoprobe with a force constant of 1.8 N/m and a resonance frequency of 23.2 kHz. The probe was scanned in air at a relative humidity of 35% to 40%.

Firstly, the formation of APhS SAM was confirmed by the ellipsometry, water contact angle and XPS measurement. The static water contact angle of the sample surface after preparation was about 60°. Its film thickness obtained by ellipsometry was ca. 0.58 nm. This thickness was considered reasonable since the chain length of the APhS molecule was estimated to be 0.6 nm by semiempirical molecular orbital calculation using the AM1 Hamiltonian. The XPS N1s spectrum of the sample seen in Fig. 8 shows that the N1s binding energy is 399.6 eV. This binding energy agrees approximately with a previously reported value (400.0 eV). These results indicated the formation of APhS SAM on the SiO₂ substrate.

To show the effect of adsorbed water, the nano-probe was scanned at the pressure of 10⁻⁶ Pa. Fig. 9 shows topographic and surface-potential images scanned at 2 and 5 V in both air and vacuum. On the basis of these images, it is obvious that the chemical reaction does not proceed in vacuum. Thus, adsorbed water is considered necessary for the chemical conversion.

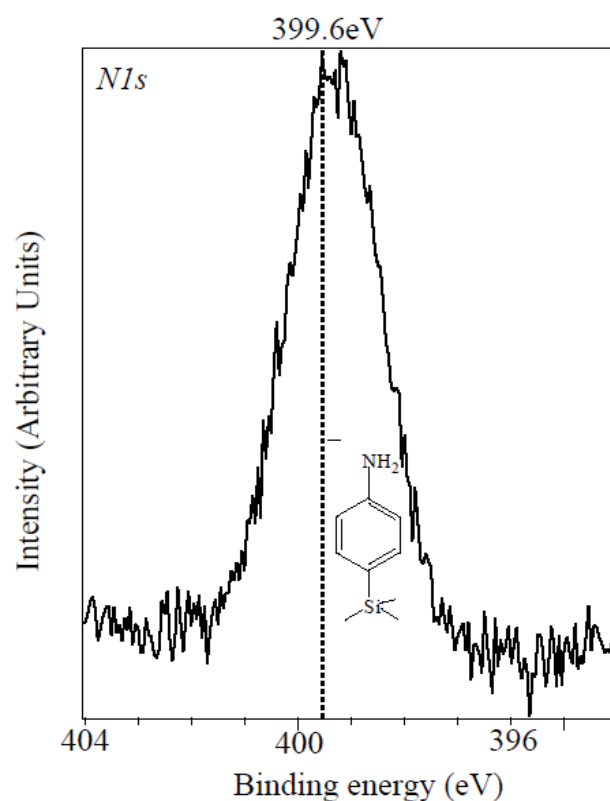


Fig. 8. XPS N1s spectrum of the Si surface covered with APhS-SAM.

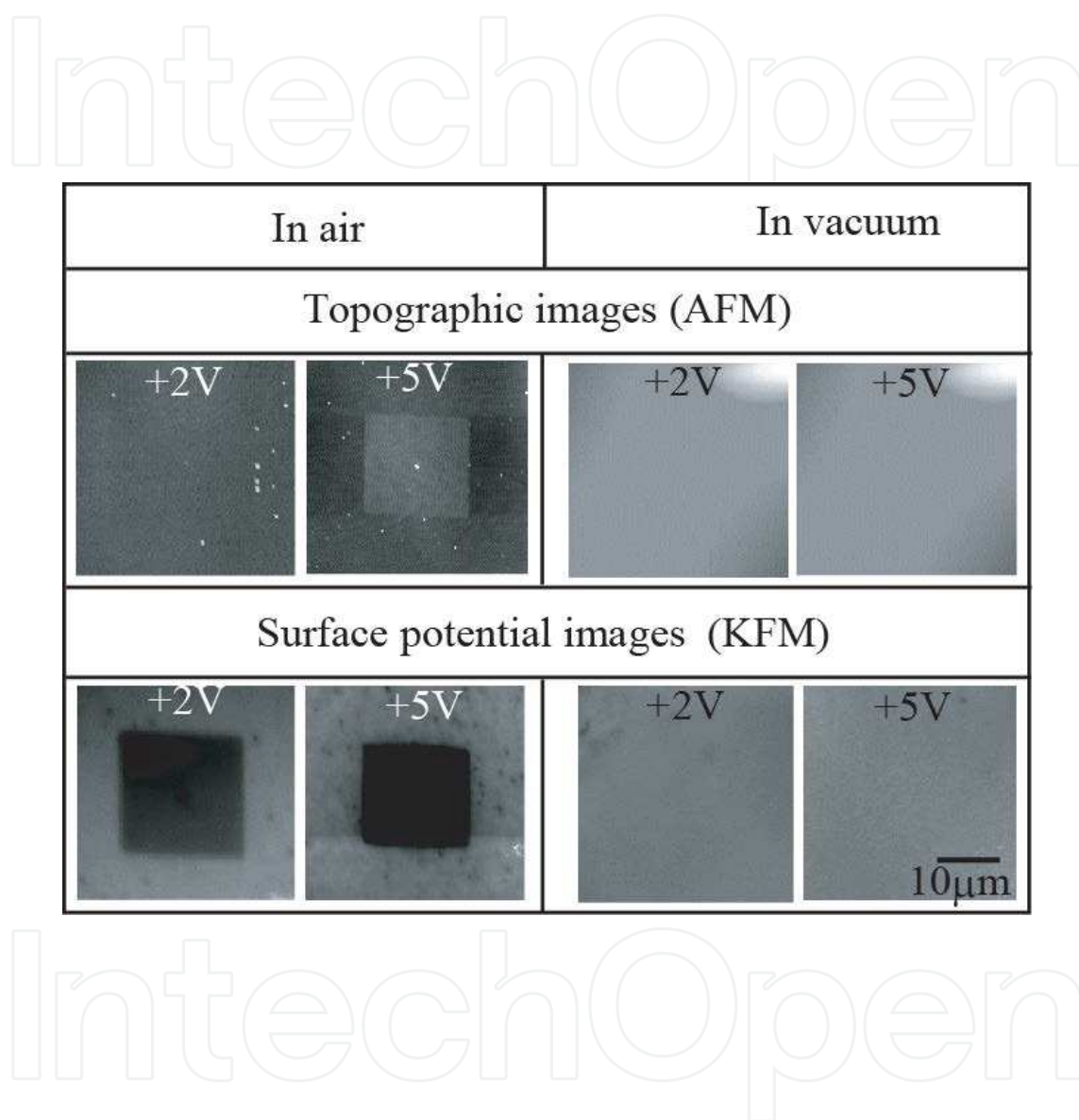


Fig. 9. Topographic and surface-potential images scanned at +2 and +5 V in air and vacuum. [N. Saito, S.H. Lee, T. Ishizaki, J. Hieda, H. Sugimura, O. Takai, Surface potential reversibility of an amino-terminated self-assembled monolayer based on nanoprobe chemistry, *J. Phys. Chem. B*, 109, 11602-11605 (2005) . Copyright@American Chemical Society (2005)]

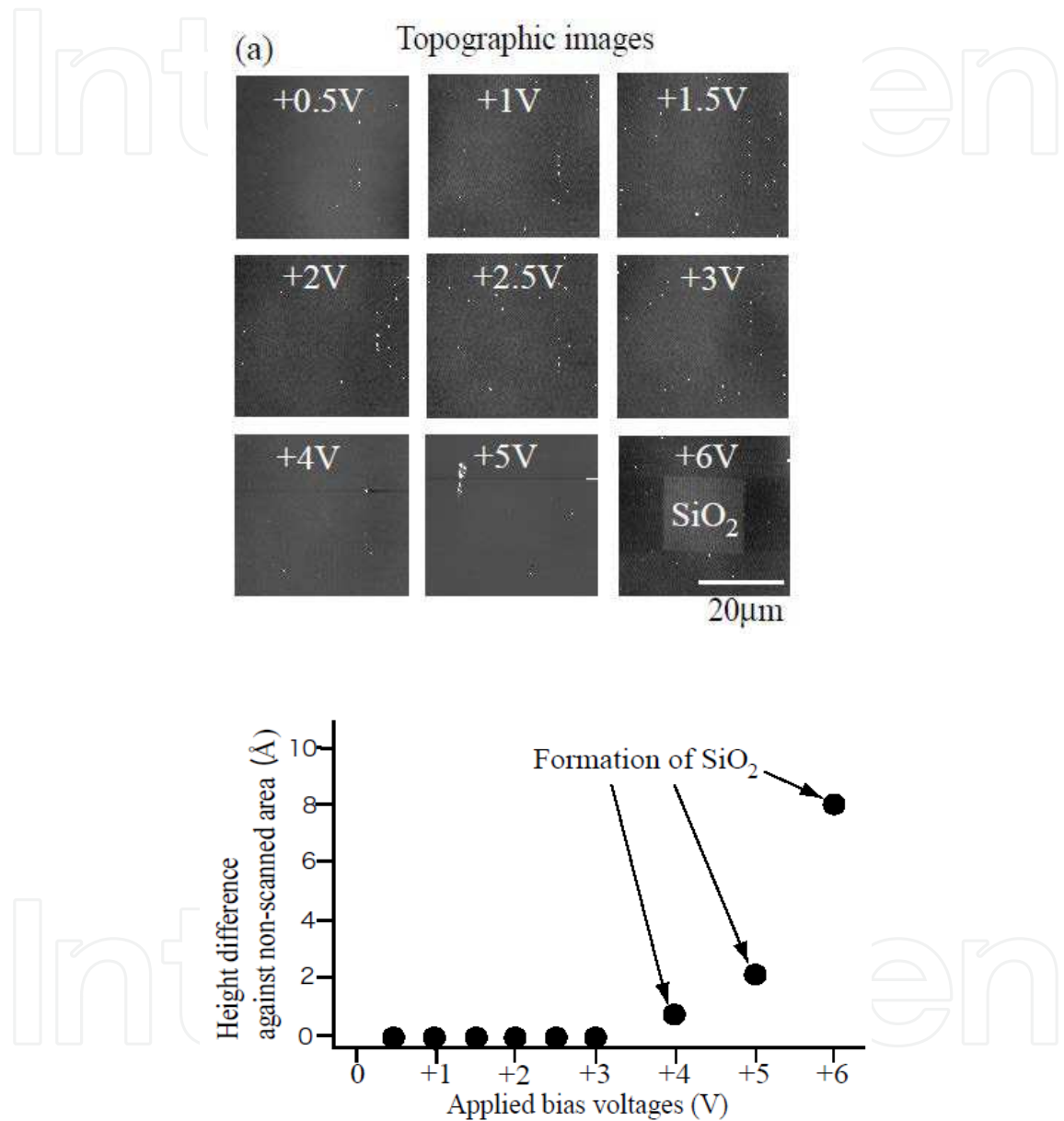


Fig. 10. (a) AFM topographic images and (b) the height difference against the non-scanned area after scanning at positive bias voltages.

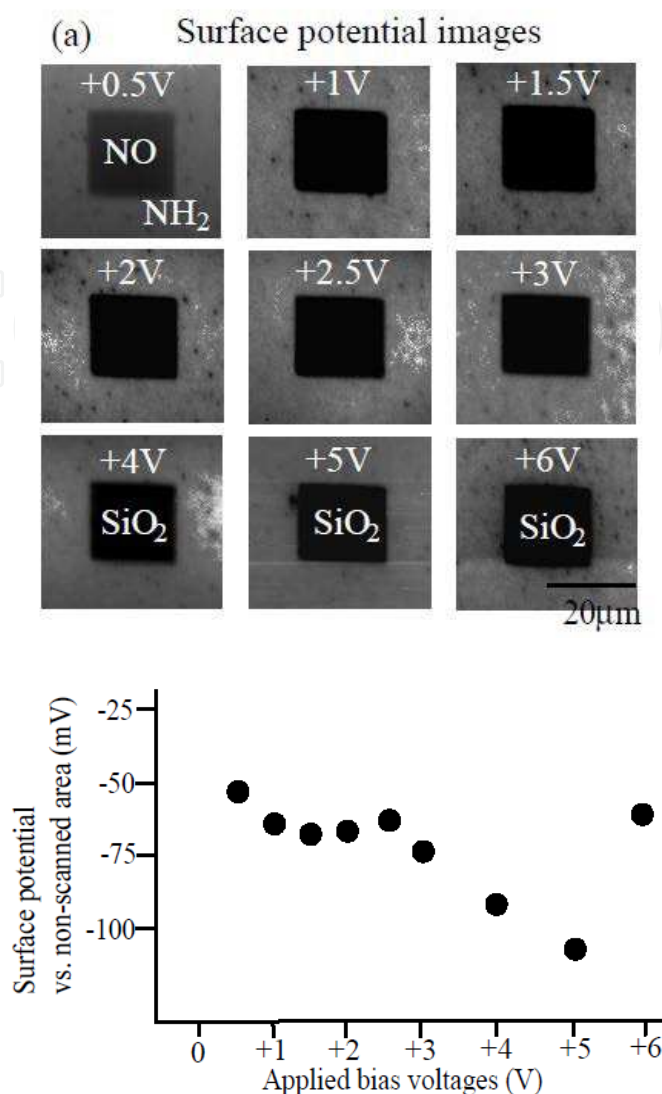


Fig. 11. (a) Surface potential images obtained by KFM and (b) the change in surface potential on the area scanned at positive bias voltages.

The nanoprobe was scanned across the sample surface over an area of $20\mu\text{m} \times 20\mu\text{m}$ at bias voltages of 0.5-6 V. Fig. 10 shows both AFM topographic images and the height difference against the nonlithographic area after scanning. A slight protuberance can be observed in the topographic images of samples scanned at the bias voltages of 4 to 6 V. This protuberance became much higher at the bias voltages of 4 to 6V. These protuberances are due to the production of SiO_2 , which resulted from the decomposition of the as-deposited APhS SAM and the oxidation of silicon. This demonstrates that there is no possibility of chemical reversibility at these bias voltages since the SAM has been damaged. Specifically, there is no possibility of surface-potential reversibility. On the other hand, no change can be observed in the topographic images of samples scanned at the bias voltages of 0.5-3 V. At these voltages, it is possible that the framework of the SAM molecules remained intact. Fig. 11 shows both surface-potential images obtained by KFM and the change in surface potential on the scanned region. The surface potential shifted negatively, which can be roughly explained by the apparent dipole moment of the SAM. The apparent dipole

moment of the untreated APhS SAM is in the direction from the sample surface to the substrate. This can explain the negative shifts of the surface potential in the scanned area. In addition, amino surfaces were converted into nitroso surface at the bias voltages of 1 V to 3 V because surface potential contrast was nearly constant. In surface potential image, the surface potential reversed with the applied bias voltage.

To confirm surface-potential reversibility, a nanoprobe scanning series was performed as follows. At first, (a) a $60\ \mu\text{m} \times 60\ \mu\text{m}$ square region was oxidized, and (b) a $20\ \mu\text{m} \times 20\ \mu\text{m}$ square region in the $60\ \mu\text{m} \times 60\ \mu\text{m}$ square region was reduced. The scan rates were 0.5 and 1.0 Hz, respectively. Fig. 12 shows illustrates of these (a) experimental processes and (b) surface potential image of scanned area. In surface potential image, the surface potential reversed with the applied bias voltage. Fig. 13 shows (a) schematic illustration of selective adsorption of carboxyl- modified fluorescent spheres after AFM lithography and (b) dark field image acquired by optical microscope after immersion of the sample in Fig. 12 in a pH 4 solution containing carboxyl-modified fluorescent spheres. The $-\text{COOH}$ and $-\text{NH}_2$ groups in the pH 4 solution were converted into $-\text{COO}^-$ and $-\text{NH}_3^+$ ion groups. Thus, the selective adsorption of fluorescent spheres onto the NH_2 regions proceeded due to attractive electrostatic interaction. In the pH 4 solution, amino-modified fluorescent spheres were repulsed in regions with $-\text{NO}$ terminated groups. Therefore, the bright and dark areas correspond to the NH_2 and NO surface, respectively. These indicated that the nitroso terminated surfaces were reconverted into amino terminated surfaces with a negative bias voltage.

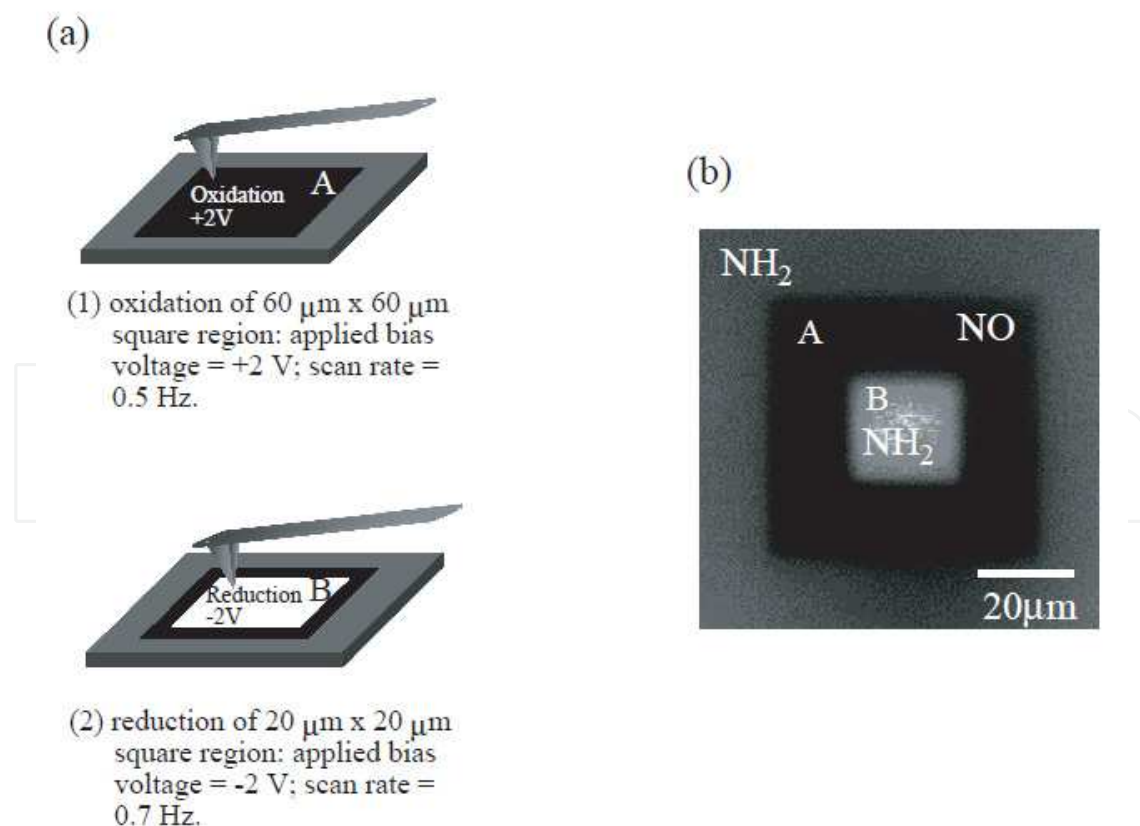
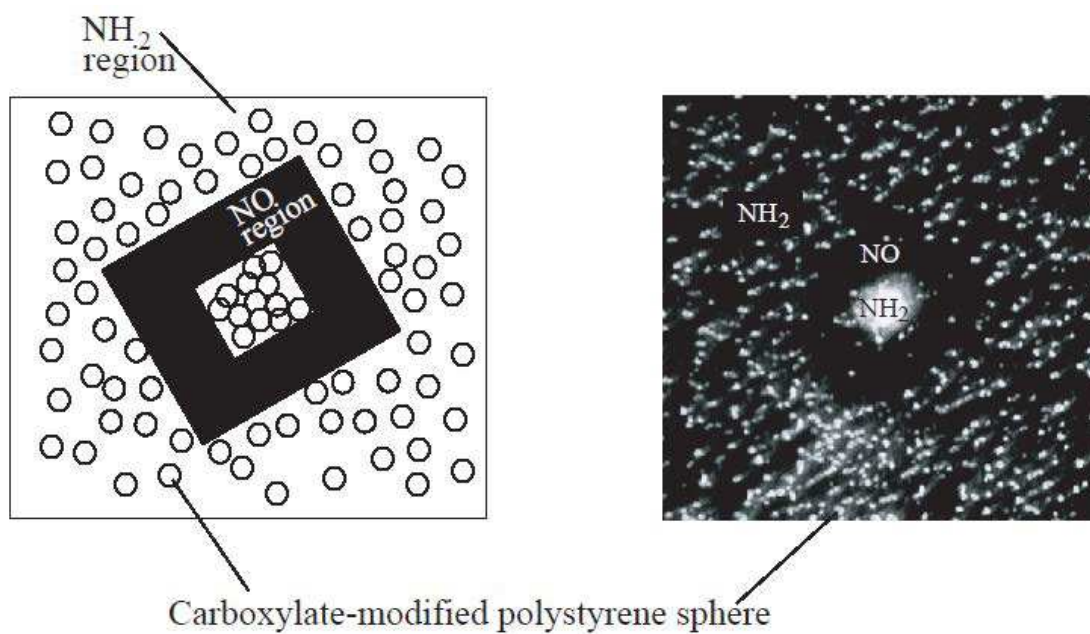


Fig. 12. (a) Schematic illustrations for a series of the lithography and (b) the obtained surface potential image.

IntechOpen



IntechOpen

Fig. 13. (a) Schematic illustration of selective adsorption of carboxylate-modified polystyrene spheres after AFM lithography and (b) dark field image acquired by optical microscope after immersion in a pH 4 solution containing carboxylate-modified polystyrene spheres, followed by successive scanning probe lithography.

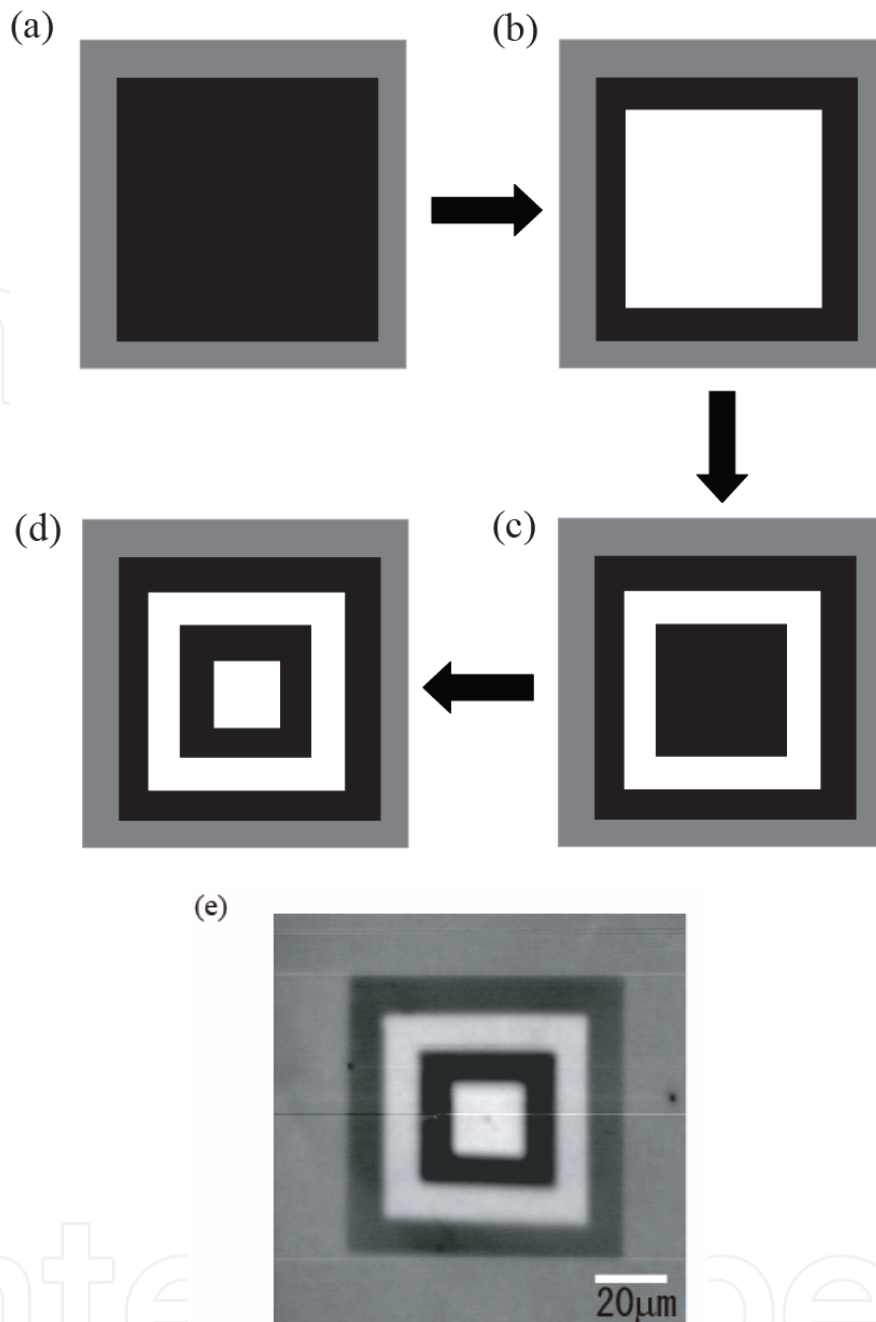


Fig. 14. Illustrations of reversibility processes ((a)-(d)) and the surface potential image of multi-scanned area (e).

In addition, we investigated the multi-reversible conversion of the APhS surface. Firstly, (a) a $80\ \mu\text{m} \times 80\ \mu\text{m}$ square region was oxidized, and (b) a $60\ \mu\text{m} \times 60\ \mu\text{m}$ square region in the $80\ \mu\text{m} \times 80\ \mu\text{m}$ square region was reduced. Moreover, (c) the $40\ \mu\text{m} \times 40\ \mu\text{m}$ square region in the $60\ \mu\text{m} \times 60\ \mu\text{m}$ square region was oxidized, and then (d) the $20\ \mu\text{m} \times 20\ \mu\text{m}$ square region the $40\ \mu\text{m} \times 40\ \mu\text{m}$ square region was reduced. The scan rates were 0.5, 0.7, 1.0, and 2.0 Hz, respectively. Fig. 14 (a) and (b) show illustrations of these experimental processes and the surface potential image of the scanned area, respectively. In the surface potential image, the surface potential reversed with the applied bias voltage. These indicated the multi-reversible conversion of amino terminated surfaces. Thus, we can control the surface-

potential reversibility on the amino-terminated SAM by controlling the applied bias voltage. This reaction formula is as follows .



Finally, by making use of this phenomenon of surface-potential reversibility, we demonstrated surface-potential memory. First, a square region $10 \mu\text{m} \times 10 \mu\text{m}$ was oxidized at the bias voltage of 2 V. Next, dotted areas in the oxidized region were selectively reduced at the bias voltage of -2 V. Finally, the $10 \mu\text{m} \times 10 \mu\text{m}$ square region was again oxidized at the bias voltage of 2 V. Fig. 15 shows the surface potential changes corresponding to (a) “writing” and (b) “erasing” with the experimental process. In Fig. 15 (a), sixteen bright areas corresponding to the chemically converted region can be observed. These sixteen areas disappeared after “erasing,” as shown in Fig. 15 (b). Although this “surface potential memory” has not yet been highly integrated, it has the potential to perform as ultra-integrated memory.

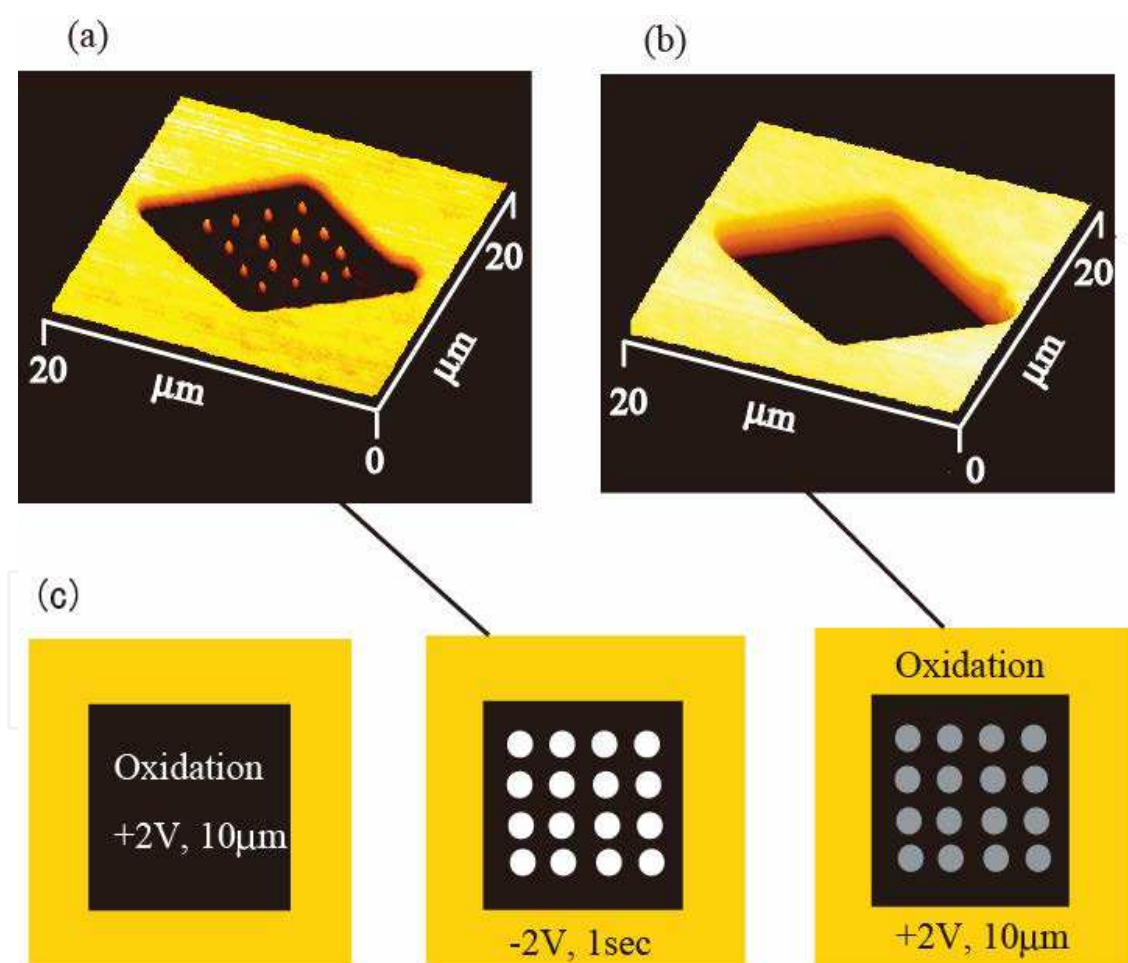


Fig. 15. Surface-potential memory: (a) “writing” state, (b) “erasing” state (c) and the experimental process.

4.1 Electrochemical lithography of 1,7-octadiene monolayers covalently linked to hydrogen-terminated silicon using scanning probe microscopy

The organic monolayer covalently attached to silicon through Si-C bond has been expected to have better chemical resistivity compared to organosilane monolayers. The Si-C interface provides a good electronic property for molecular devices constructed on the silicon. In particular, the construction of hybrid organic- molecule/silicon devices is a promising approach for the future molecular devices. To realize such devices, it is vital to establish the fabrication technology for microstructure of the organic monolayer. The electrochemical SPL is performed through the water column condensed between the tip of SPM and the substrate surface. This water column can be used as a minute electrochemical cell. When the bias voltage is applied, a redox reaction proceeds on the substrate surface. Through reversible chemical SPL, we successfully controlled this redox reaction so that an NH_2 -terminated organosilane monolayer surface was converted into an NO-terminated surface. However, this organosilane monolayer suffered from electrical defects due to the presence of SiO_x . A 1,7-octadiene (OD) monolayer was directly formed on a hydrogen-terminated silicon surface by radical reaction. In this section, we report the electrochemical conversion of the vinyl-terminated groups on an OD monolayer induced by a nanoprobe.

Si (111) with electrical resistivity of 10.0-20.0 Ω/cm was used as for the substrates. Fig. 16 shows schematic illustrations of the experimental process. The substrates were cleaned in piranha solution ($\text{H}_2\text{SO}_4 : \text{H}_2\text{O}_2 = 3 : 1$) at 100 $^\circ\text{C}$ for 10 min and rinsed in ultrapure water. They were then etched for 15 min by immersing in 40 % aqueous ammonium fluoride solution (NH_4F). The surface was hydrogen-terminated and silicon oxide was removed by this immersion. The OD monolayer was prepared by the liquid phase method. The substrates were immersed in OD solution at 120 $^\circ\text{C}$ for 1h. After immersion, the samples were cleaned in toluene, acetone, ethanol and rinsed in ultrapure water.

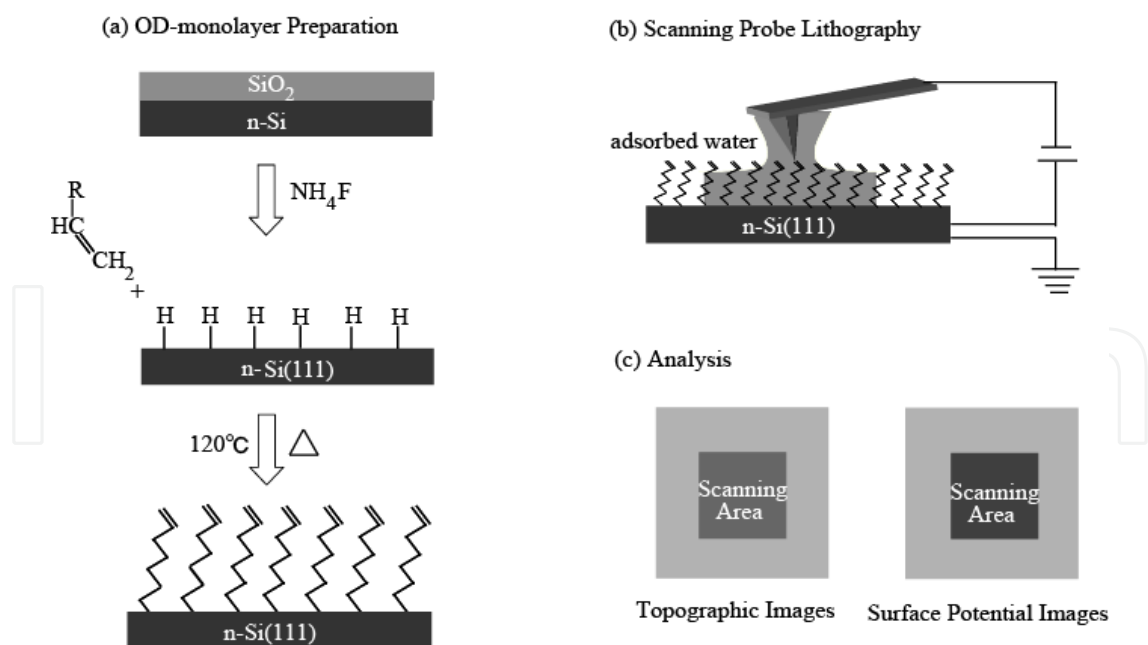


Fig. 16. Schematic illustrations of the experimental process: (a) preparation of the OD-monolayer, (b) electrochemical scanning probe lithography and (c) chemical conversion analysis. [SH. Lee, T. Ishizaki, N. Saito, O. Takai, Electrochemical Soft Lithography of an 1,7-octadiene Monolayer Covalently Linked to Hydrogen-Terminated Silicon using Scanning Probe Microscope, *Surf. Sci.*, 601, 4206-4211 (2007). Copyright@ELSEVIER (2007)]

Fig. 17 (a) shows the XPS Si 2p spectra of silicon substrate surfaces before and after the immersion in 40 % aqueous ammonium fluoride solutions (NH_4F). In the spectrum of the sample surface before the immersion, the peak at 104 eV attributed to SiO_2 was observed, while no appreciable peak related to the oxide was observed in the spectrum after the immersion. This indicates that the native oxide layer on the silicon substrate is completely removed after the immersion. Fig. 17 (b) show the AFM topographic image of the silicon substrate surface. The AFM image has flat terraces with the steps for silicon one-atom. The distance and the height difference between steps were evaluated to be 180 nm and 0.32 ± 0.03 nm, respectively, as shown in Fig. 17 (b). These results reveal that the silicon surfaces are terminated with hydrogen. In order to deposit the OD monolayers, the substrate was immersed in the OD solution heated at 120 °C for 1 h. After the immersion, the water contact angle of the OD monolayers became saturated at approximately 80° at the reaction time of 1 hour. Furthermore, the film thickness of 1.2 nm corresponded approximately to the distance from Si to $-\text{CH}_2$ end groups in the precursor, as determined by ellipsometry. Fig. 17 (c) shows the topographic image of the OD monolayer surface. The distance and the height difference between steps, as shown in Fig. 17 (c), were 120 nm and 0.28 ± 0.03 nm, respectively. These values are well in agreement with that of hydrogen-terminated silicon surface. The OD monolayers were stably attached to the hydrogen-terminated Si surfaces, since the parallel monoatomic steps were observed on the OD molecule. This means that the OD molecule was deposited at a monolayer on the substrate. These surfaces are very stable and can be stored for several weeks without any change in the topographic properties.

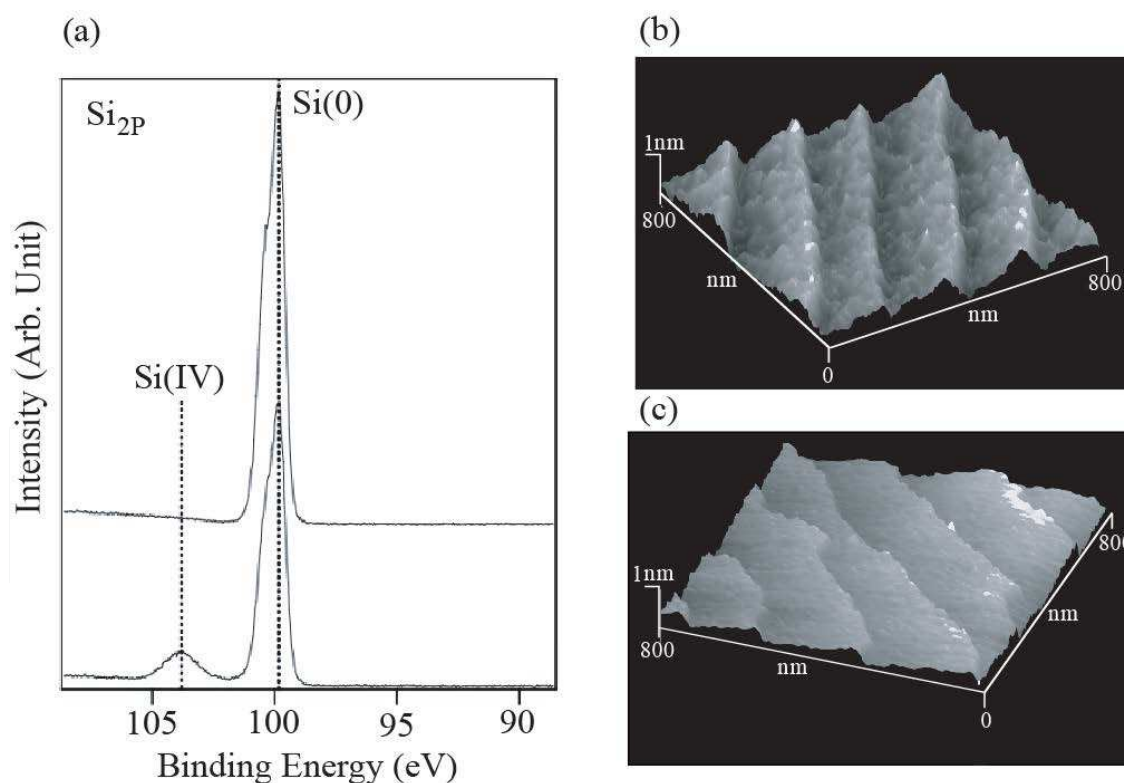


Fig. 17. (a) Si2p XPS spectra of the Si(111) surface after and before etching in 40% NH_4F , (b) AFM image (800nm×800nm) of a H-terminated Si(111) surface, (c) AFM image (800nm×800nm) of a OD-monolayer surface [SH. Lee, T. Ishizaki, N. Saito, O. Takai, Local Generation of Carboxyl Groups on an Organic Monolayer through Chemical conversion using Scanning Probe Anodization: Mater. Sci. Eng. C, 27, 1241-1246 (2007) Copyright@ELSEVIER (2007)]

The OD monolayers were selectively oxidized in air through the photomask by vacuum ultraviolet (VUV) light irradiation for 10 min. The areas irradiated were converted into -COOH groups due to photochemical oxidation, thus dividing the small surface into distinct -CH₂ and -COOH end groups regions. Fig. 18 (a) shows the XPS C1s spectra of OD monolayer surfaces before and after the irradiation. Its peak of 289.6 eV is assigned to the carboxyl group. Fig. 18 (b) shows the surface potential image (KFM) of the OD monolayer. The dark and bright regions correspond to the CPD images of low and high surface potential, respectively. In this figure, the surface potential for the irradiated OD monolayer surfaces was 20 mV lower than that of the unirradiated surfaces. The change of the surface potential indicates that -CH₂ end groups on the OD monolayer were chemically converted into -COOH end groups. The end groups of the OD monolayers were confirmed by the selective adsorption of amino-modified fluorescence spheres in a pH 4 solution. The -COOH and -NH₂ groups in the pH 4 solution were converted into -COO⁻ and -NH₃⁺ ion groups, so that the selective adsorption of fluorescence spheres on to the substrate proceeded due to their attractive interaction to the surface. Under this pH condition, the regions of -CH₂ end groups on the surface were not negatively charged and the amino-modified polystyrene fluorescence spheres did not adsorb onto it. Fig. 18 (c) shows an image acquired by dark field microscopy of the micropatterned CH₂ / COOH sample after immersion. The lighter areas between the dark rectangular regions correspond to the COOH terminated regions. This dark-field image indicates that amino-modified polystyrene fluorescence spheres selectively adsorbed on the -COOH end group regions since scattered light due to surface roughness can be observed. From these results, we determined that an -CH₂ end group had been successfully converted into the COOH terminated surface through chemical lithography, i.e., photolithography.

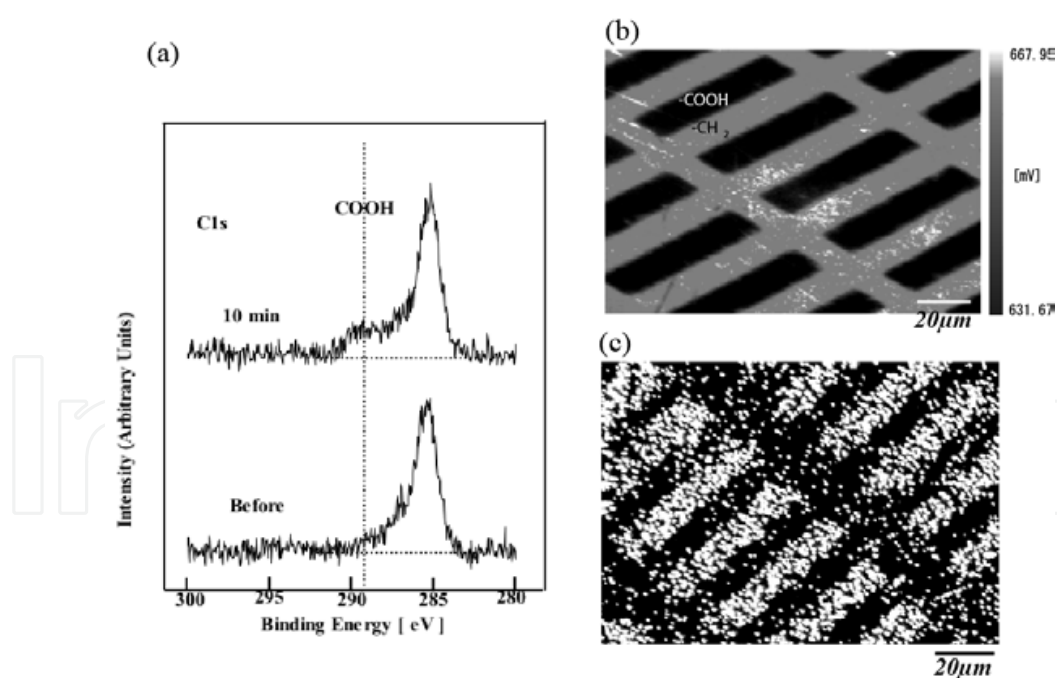


Fig. 18. (a) C1s XPS spectra for VUV irradiation of 0 and 10min, (b) KFM image (150µm×150µm) of OD-monolayer irradiated for 10min, (c) optical microscope image of the irradiated OD-monolayer which adsorbed amino terminated particles.[SH. Lee, T. Ishizaki, N. Saito, O. Takai, Local Generation of Carboxyl Groups on an Organic Monolayer through Chemical conversion using Scanning Probe Anodization: Mater. Sci. Eng. C, 27, 1241-1246 (2007). Copyright@ELSEVIER (2007)]

A gold-coated probe was scanned in air on OD monolayers at the bias voltage of 1 V and the scanning rate of 2 Hz. The areas scanned were a square, 20 μm on a side. Fig. 19 (a) and (b) shows the topographic and the surface potential images, respectively. The surface potential for the area scanned was 20 mV more negative than that of the area non-scanned and no change was observed in the topographic images. The value of surface potential difference between the scanned and non-scanned areas by SPL is well in agreement with that by photo oxidation, i.e., VUV light. These results indicate that the scanned OD monolayer surfaces are completely oxidized and chemically converted into COOH terminated surfaces without decomposition of the OD monolayer and siloxane networks. In order to verify that the chemical conversion with SPL was electrochemically proceeded on the areas scanned through the water column, the SPL was carried out in vacuum. The conditions were as follows: the bias voltage : 1 V, the pressure : 10^{-4} Pa, the scanned rate : 2 Hz, and the scanned areas : a square of 20 μm on a side. Fig. 20 shows the topographic and the surface potential images on the scanned area. In both images, no change was observed. This means that the chemical conversion on the scanned areas does not proceed under such a condition. Therefore, we can conclude that the chemical conversions with SPL are based on electrochemical reactions through the water column.

Electrochemical SPL was performed on the OD monolayer at the scanning rate of 2 Hz and at bias voltages of -3 V to 3 V. Fig. 21 shows representative surface potential images, topographic images, the changes in surface potential, and the height difference against the non-lithographic regions. In topographic images, no change in height difference was observed at any of the bias voltages. This indicates that the scanning caused no change in microscopic morphology under these conditions. On the other hand, the surface potential changed remarkably. The dark and bright regions in the surface potential images correspond to low and high surface potential regions, respectively. When the bias voltage was positively applied, oxidation proceeded on the substrate. At the positive bias voltage, the scanned regions were oxidized and showed lower surface potential than the unscanned areas. The surface potential contrast was nearly constant at approximately -18 mV at bias voltages of 1 V to 2 V. However, the surface potential contrast at bias voltages of 2 V to 3 V gradually decreased in proportion to voltage evolution.

On the other hand, the surface potential contrast at negative bias voltages gradually increased in proportion to voltage evolution. The surface potential contrast at bias voltages of 0 V to -1 V was negative, indicating that some oxidation proceeded under these conditions. This was due to the difference in contact potential between the Au-coated probe and the Si substrate. The surface potential constant was positive at bias voltages from -1.5 V to -3 V. This change in surface potential indicates that reduction reactions occurred on the substrate surface due to the applied negative bias voltage. Considering these AFM and KPFM results, the electrochemical conversion of the vinyl-terminated groups is believed to have been governed by the applied bias voltage.

Using XPS, we investigated the conversion of vinyl terminated groups at each bias voltage. Fig. 22 (a) and (b) show XPS Si2P and C1s spectra for sample surfaces after probe-scanning at bias voltages of 1 V and 3 V. The C1s spectrum in Fig. 22 (b) shows an additional peak from -COOH groups at 288.5 eV at the bias voltage of 1 V, but not at 3 V. In addition, a silicon oxide peak at 103.4 eV can be seen in Fig. 22 (a) at the bias voltage of 3 V, but not at 1 V. The intensity of the alkyl chain peak in Fig. 22 (b) at the bias voltage of 3 V was observed to be lower than that at 1 V. These XPS results indicate that the vinyl functional groups were oxidized and converted into carboxyl groups at the bias voltage of 1 V. The surface potential

of the carboxyl surface was lower than that of the vinyl-terminated surface because the carboxyl groups had more negative dipole moment. This agrees with the KFM results. In addition, OD molecules on the sample surface were decomposed and silicon oxide was formed at the bias voltage of 3 V. However, the fact that there was no change of AFM morphology at the bias voltage of 3 V was probably due to the formation of “depthless” silicon oxide, that is, the partial decomposition of OD molecules, and to the effect of absorbed water on the sample surface.

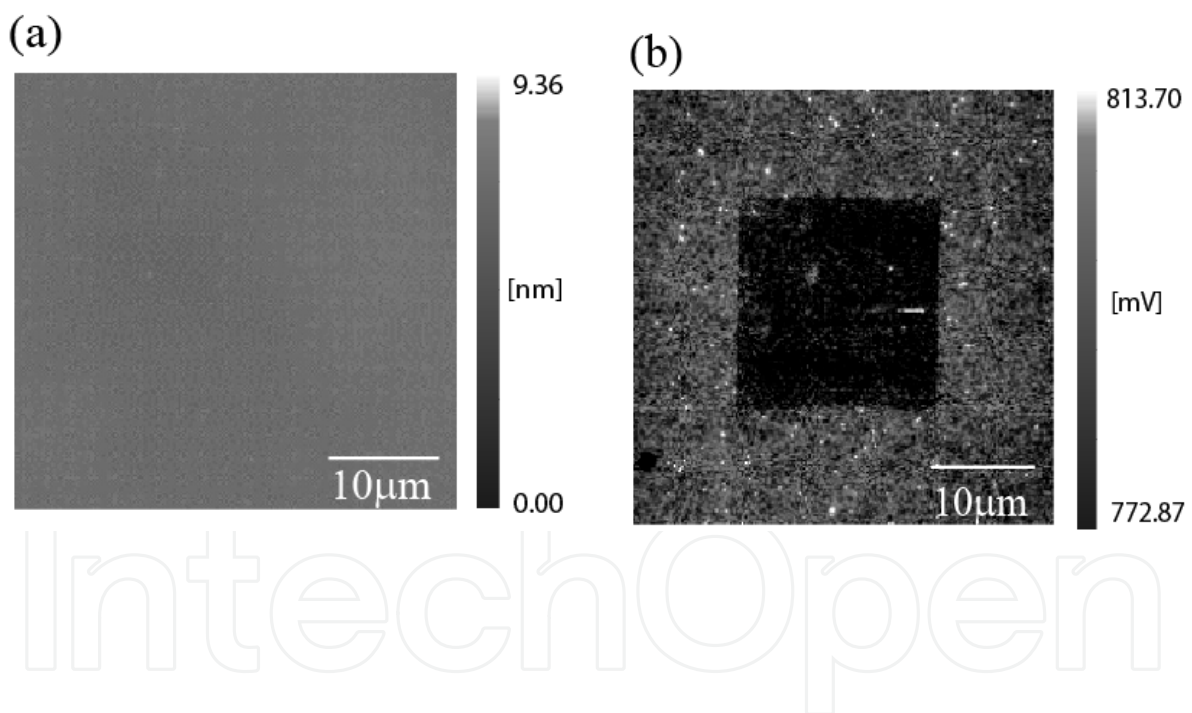
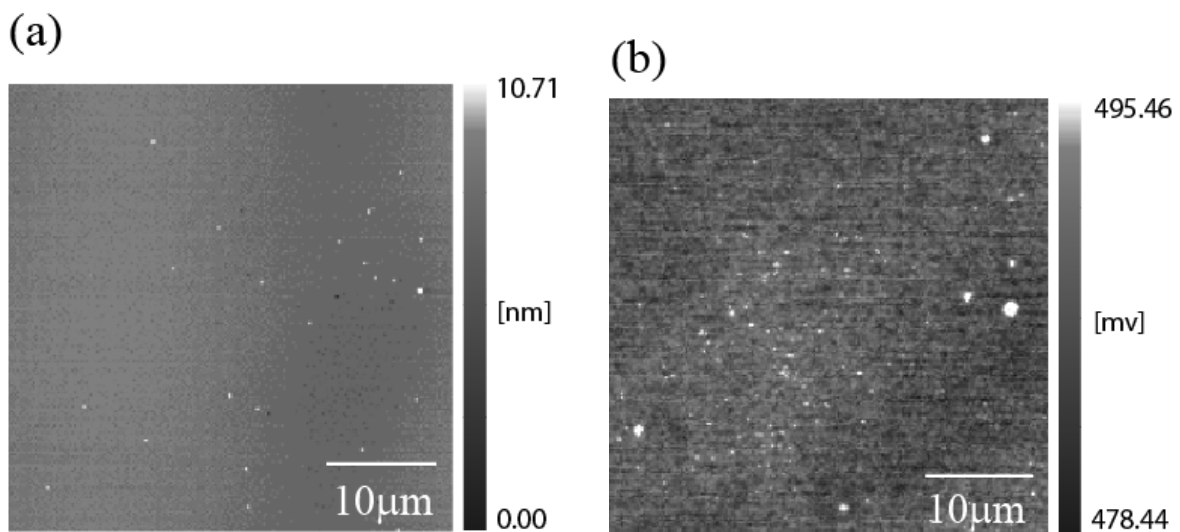


Fig. 19. (a) Topographic images and (b) surface potential image after the scanning at the rate of 2Hz. [SH. Lee, T. Ishizaki, N. Saito, O. Takai, Local Generation of Carboxyl Groups on an Organic Monolayer through Chemical conversion using Scanning Probe Anodization: Mater. Sci. Eng. C, 27, 1241-1246 (2007). Copyright@ELSEVIER (2007)]

IntechOpen



IntechOpen

Fig. 20. (a) Topographic image and (b) surface potential image after the scanning in vacuum.[SH. Lee, T. Ishizaki, N. Saito, O. Takai, Local Generation of Carboxyl Groups on an Organic Monolayer through Chemical conversion using Scanning Probe Anodization: Mater. Sci. Eng. C, 27, 1241-1246 (2007). Copyright@ELSEVIER (2007)]

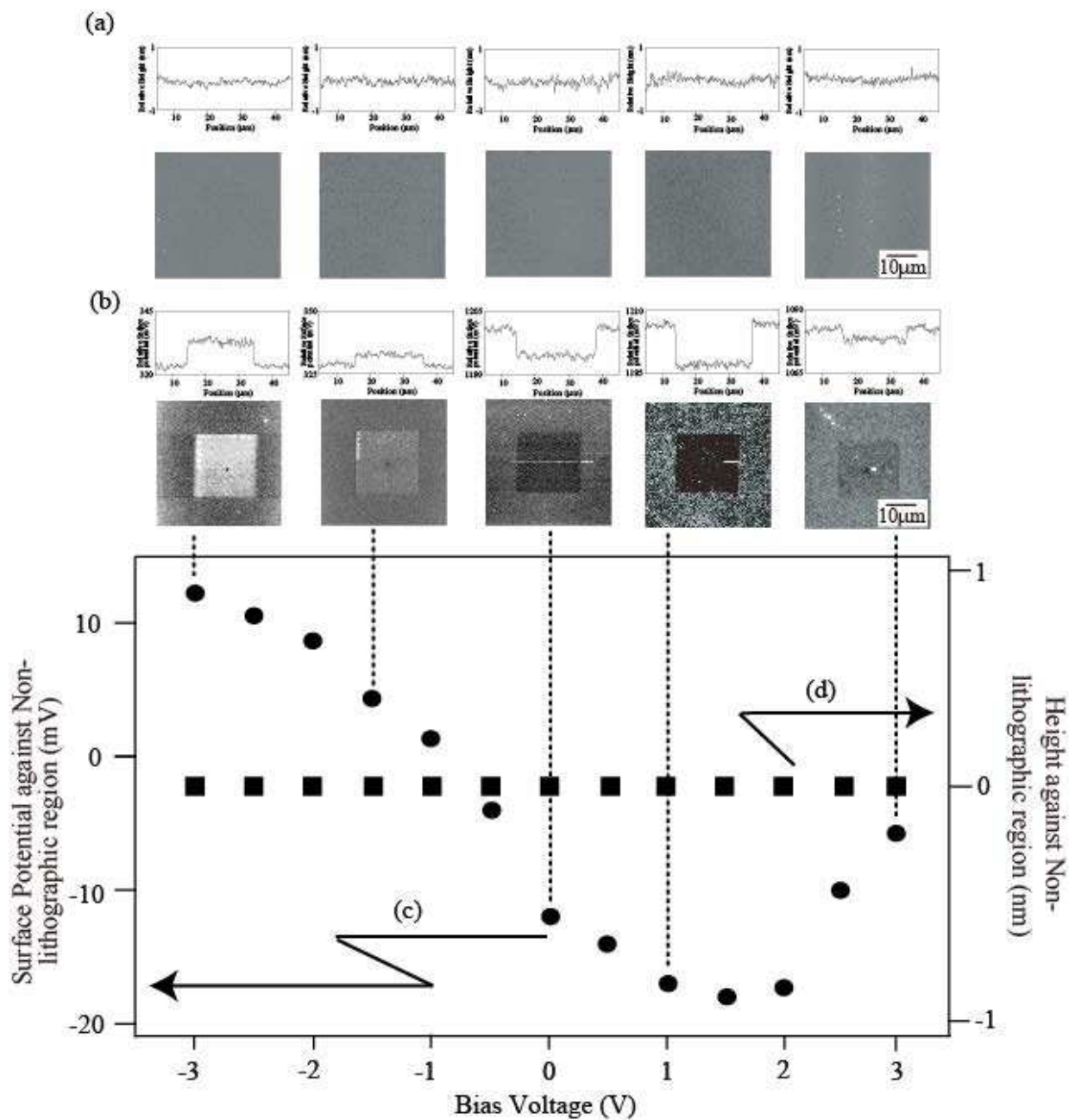


Fig. 21. (a) Representative topographic images, (b) representative surface potential images, (c) change of surface potential against non-lithographic regions; and (d) height difference against non-lithographic regions. Electrochemical SPL was performed at bias voltages of -3V to 3V. [SH. Lee, T. Ishizaki, N. Saito, O. Takai, Electrochemical Soft Lithography of an 1,7-octadiene Monolayer Covalently Linked to Hydrogen-Terminated Silicon using Scanning Probe Microscope, *Surf. Sci.*, 601, 4206-4211 (2007). Copyright@ELSEVIER (2007)]

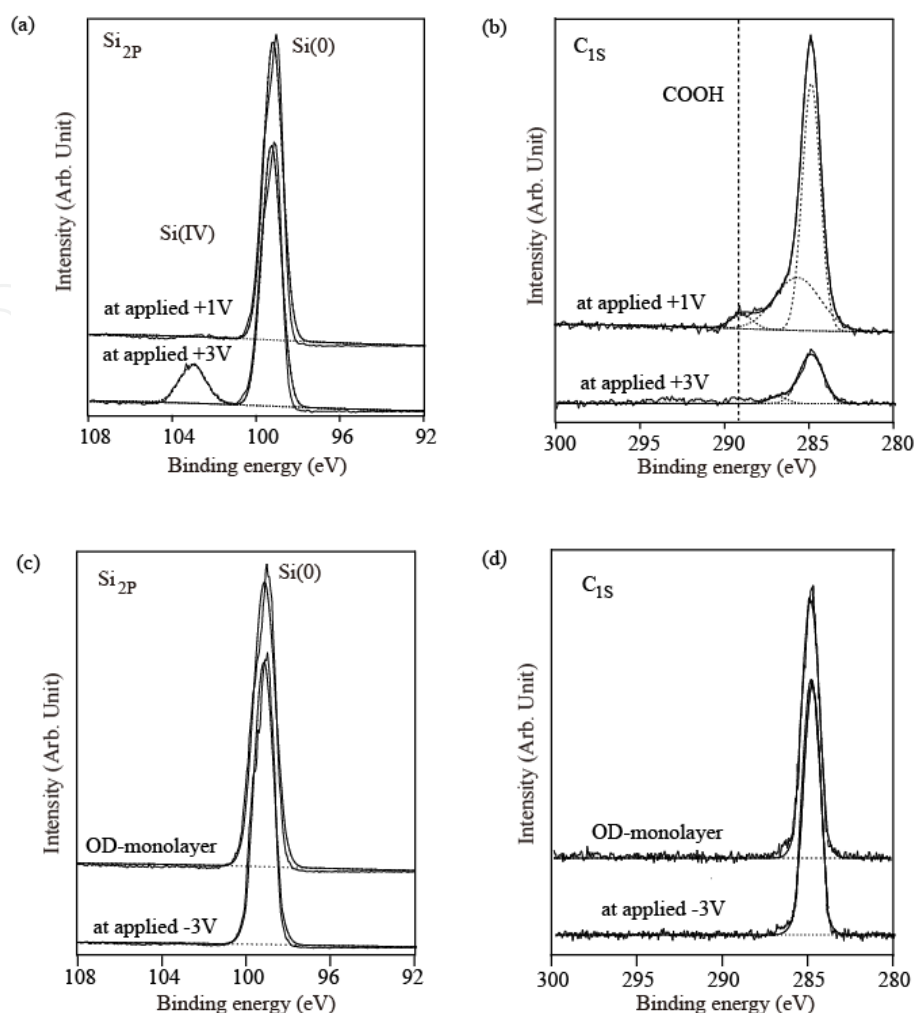


Fig. 22. (a) XPS Si_{2p} spectra and (b) XPS C_{1s} spectra of sample surfaces after probe-scanning at bias voltages of 1V and 3V. (c) XPS Si_{2p} spectra and (d) XPS C_{1s} spectra of an OD-monolayer surface and a sample surface after probe-scanning at the bias voltage of -3V. [SH. Lee, T. Ishizaki, N. Saito, O. Takai, Electrochemical Soft Lithography of an 1,7-octadiene Monolayer Covalently Linked to Hydrogen-Terminated Silicon using Scanning Probe Microscope, *Surf. Sci.*, 601, 4206-4211 (2007). Copyright@ELSEVIER (2007)]

Fig. 22 (c) and (d) show XPS Si_{2p} and C_{1s} spectra of an unscanned OD-monolayer surface and a sample surface scanned at the bias voltage of -3 V. In the C_{1s} XPS spectrum in Fig. 22 (d), the intensity of the alkyl chain peak for the surface scanned at the bias voltage of -3 V was the same as that for the OD monolayer. The silicon oxide peaks in the Si_{2p} spectra were not observed in all cases [Fig. 22 (a) and (c)]. These XPS results indicate that OD molecules were not decomposed at negative bias voltage. We believe that the vinyl functional groups were reduced and converted into cyclobutane rings. No peak for these cyclobutane rings was observed in the C_{1s} spectra since such a peak is generally weak. However, in view of the AFM and KFM results, we consider that cyclobutane rings form in the same manner as they are known to in photochemical and thermal reactions.

Fig. 23 shows a schematic illustration of the mechanism of electrochemical SPL on the OD monolayer. In this Section, two factors were considered: the alkyl radical reaction from frictional heat due to the probe scanning, and the redox reaction on the sample surface

caused by polarization due to the applied bias voltage. First, alkyl radicals were formed by frictional heat. Next, the redox reaction occurred on the sample surface in the radical atmosphere. With positive bias voltages, the oxidation reaction easily occurred on the sample surface due to polarization in adsorbed water. Thus, the conversions on the sample surface were governed by the oxidation reaction. The vinyl-terminated groups of the OD monolayer were converted into carboxyl groups at positive bias voltage. However, the reduction reaction on the sample surface rarely occurred at negative bias voltages because the dissolved oxygen was preferentially reduced in adsorbed water. Thus, in this case, the surface reaction was governed by alkyl radicals. The formation of cyclobutane rings was considered to have occurred due to alkyl radical combinations at the negative bias voltage.

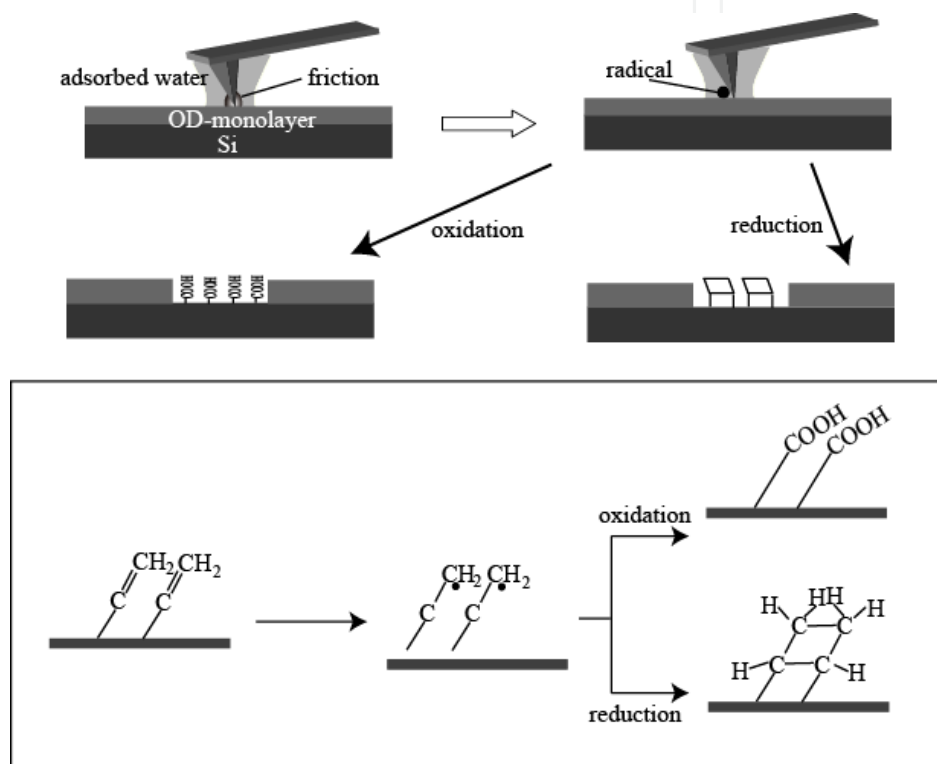


Fig. 23. Schematic illustration of the redox reaction induced by electrochemical SPL [SH. Lee, T. Ishizaki, N. Saito, O. Takai, *Electrochemical Soft Lithography of an 1,7-octadiene Monolayer Covalently Linked to Hydrogen-Terminated Silicon using Scanning Probe Microscope*, *Surf. Sci.*, 601, 4206-4211 (2007). Copyright@ELSEVIER (2007)].

In support of the SPM and XPS results, the oxidized groups of the OD monolayer were confirmed by the selective adsorption of amino-modified fluorescent spheres. The $-\text{COOH}$ and $-\text{NH}_2$ groups in the pH 4 solution were converted into $-\text{COO}^-$ and $-\text{NH}_3^+$ ion groups. Thus, the selective adsorption of fluorescent spheres onto the COOH regions proceeded due to attractive electrostatic interaction. In the pH 4 solution, regions with vinyl terminated groups were not negatively charged, and the amino-modified polystyrene fluorescent spheres were repulsed. Fig. 24 (a) shows the mechanism of this selective adsorption of the amino-modified fluorescence spheres. Fig. 24 (b) shows a dark field image of samples scanned at the bias voltage of 1 V after immersion in the solution of amino-modified fluorescent spheres. The bright areas correspond to the areas scanned at the bias voltage of 1 V which site-selectively adsorbed the fluorescent spheres. This confirms that vinyl

terminated groups of the OD monolayer were converted into COOH terminated groups by scanning at the applied bias voltage of 1 V.

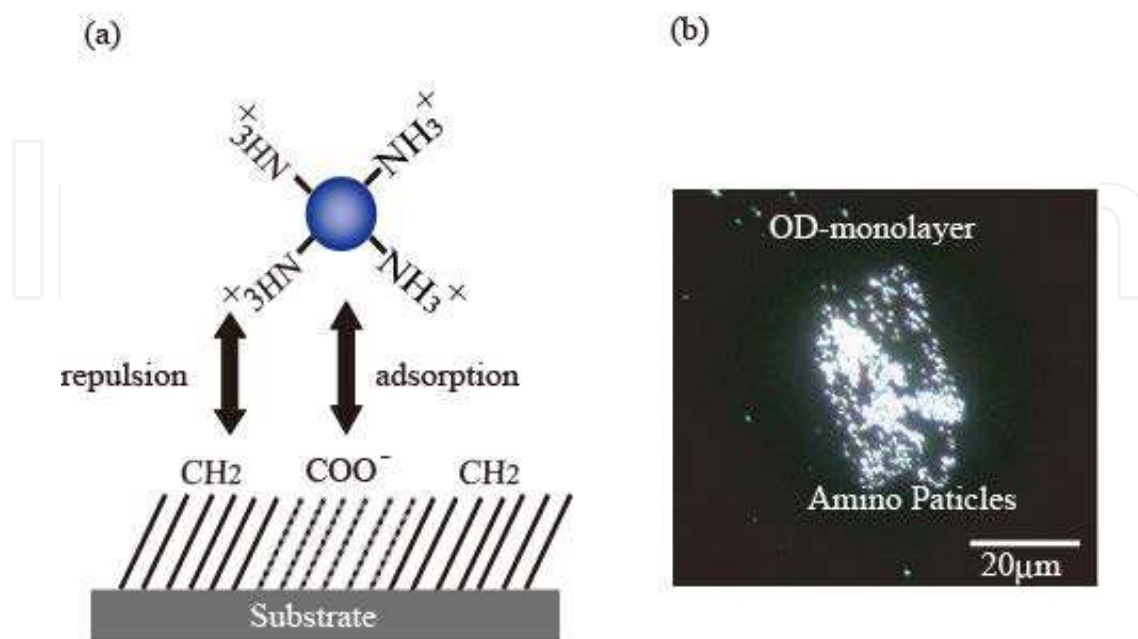


Fig. 24. (a) Selective adsorption of amino-modified fluorescent spheres on a surface scanned at the bias voltage of 1V; (b) dark field image of a patterned surface after immersion in a pH 4 solution containing amino-modified fluorescent spheres [SH. Lee, T. Ishizaki, N. Saito, O. Takai, *Electrochemical Soft Lithography of an 1,7-octadiene Monolayer Covalently Linked to Hydrogen-Terminated Silicon using Scanning Probe Microscope*, *Surf. Sci.*, 601, 4206-4211 (2007). Copyright@ELSEVIER (2007)].

5. Conclusion

In this chapter, we introduced the chemical conversion of functional groups on the organic monolayer by electrochemical SPL. The three-dimensional nanostructures of silicon oxide were successfully fabricated by decomposing the 1-decane monolayer and subsequent oxidizing the hydrogen-terminated Si surfaces via anodization SPL. The size and reproducibility of oxide nanoline structures were greatly dependent on the sorts of probes for anodization SPL. In the case of Au-coated Si and uncoated Si probes, the obtained nanoline structures were changed with the scanning rates and the applied bias voltages. On the other hand, the nanotexture fabrication using the diamond-coated probe showed one of the finest structures (15 nm nanoline) and highly reproducibility even though any fabrication conditions such as scanning rate and applied bias voltage are used in the anodization SPL. The amino surface on SAM was oxidized and converted into a nitroso surface at bias voltages of 0.5 to 3 V. The functional groups on APhS SAM were reversibly converted by controlling the applied bias voltage. It was also demonstrated that the surface-potential memory was based on surface potential reversibility. In addition, the vinyl-terminated groups of the OD monolayer were site-selectively oxidized and chemically converted into carboxyl groups at bias voltages of 1 to 2 V. OD molecules on the sample surface were decomposed and silicon oxide was formed at bias voltages greater than 3 V. On the other hand, CH₂-terminal groups were converted into

cyclobutane rings at bias voltages of less than -1.5 V. Recently, the research into applications of SAMs has progressed rapidly because of their ability to modify surfaces functionally and provide hydrophobicity, hydrophilicity, or biocompatibility. However, the reproducibility of the formation of SAMs is difficult. In this chapter, the formation mechanism of SAMs has been studied for high reproducibility. The control of surface properties by fabrication of micro/nanosized domains composed of SAMs is expected to be applied in the field of biomaterials. In addition, electrochemical SPL is also expected to be applied to various devices.

6. References

- Hayashi, K.; Saito, N.; Sugimura, H.; Takai, O. & Nagairo, N. (2002). Regulation of the Surface Potential of Silicon Substrates in Micrometer Scale with Organosilane Self-Assembled Monolayers. *Langmuir*, Vol.8, No.20 (September 2002), pp. 7469-7472, ISSN 0743-7463.
- Hong, L.; Sugimura, H.; Furukawa, T. & Takai, O. (2003). Photoreactivity of Alkylsilane Self-Assembled Monolayers on Silicon Surfaces and Its Application to Preparing Micropatterned Ternary Monolayers. *Langmuir*, Vol.19, No.6 (February 2003), pp. 1966-1069, ISSN 0743-7463.
- Saito, N.; Wu, Y.; Hayashi, K.; Sugimura, H. & Takai, O. (2003). Principle in Imaging Contrast in Scanning Electron Microscopy for Binary Microstructures Composed of Organosilane Self-Assembled Monolayers. *The Journal of Physical Chemistry B*, Vol.107, No.3 (December 2002), pp. 664-667, ISSN 1089-5647.
- Hahn, J. & Webber, S. E. (2004). Graphoepitaxial Deposition of Cationic Polymer Micelles on Patterned SiO₂ Surfaces. *Langmuir*, Vol.20, No.4 (January 2004), pp. 1489-1494, ISSN 0743-7463.
- Kidoaki, S. & Matsuda, T. (1999). Adhesion Forces of the Blood Plasma Proteins on Self-Assembled Monolayer Surfaces of Alkanethiolates with Different Functional Groups Measured by an Atomic Force Microscope. *Langmuir*, Vol.15, No.22 (September 1999), pp. 7639-7646, ISSN 0743-7463.
- Harnett, C. K.; Satyalakshmi, K. M. & Craighead, H. G. (2001). Bioactive Templates Fabricated by Low-Energy Electron Beam Lithography of Self-Assembled Monolayers. *Langmuir*, Vol.17, No.1 (December 2000), pp. 178-182, ISSN 0743-7463.
- Kaholek, M.; Lee, W. K.; LaMattina, B.; Caster, K. C. & Zauscher, S. (2004). Fabrication of Stimulus-Responsive Nanopatterned Polymer Brushes by Scanning-Probe Lithography. *Nano Letters*, Vol.4, No.2 (January 2004), pp. 373-376, ISSN 1530-6984.
- Blackledge, C.; Egebreton, D. A. & McDonald, J. D. (2000). Nanoscale Site-Selective Catalysis of Surface Assemblies by Palladium-Coated Atomic Force Microscopy Tips: Chemical Lithography without Electrical Current. *Langmuir*, Vol.16, No.22 (September 2000), pp. 8317-8323, ISSN 0743-7463.
- Tello, M.; García, F. & García, R. (2002). Linewidth Determination in Local Oxidation Nanolithography of Silicon Surfaces. *Journal of Applied Physics*, Vol.92, No.7 (September 2002), pp. 4075-4080, ISSN 1089-7550.

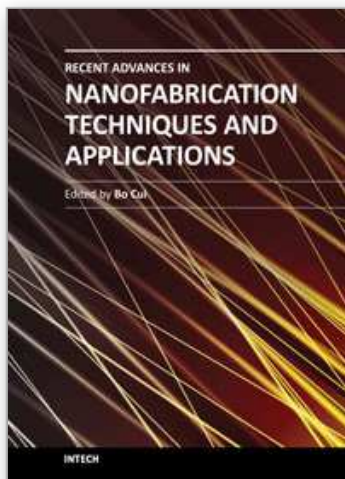
- Liu, S.; Maoz, R.; Schmid, G. & Sagiv, J. (2002). Template Guided Self-Assembly of [Au₅₅] Clusters on Nanolithographically Defined Monolayer Patterns. *Nano Letters*, Vol.2, No.10 (August 2002), pp. 1055-1060, ISSN 1530-6984.
- Jang, C. H.; Stevens, B. D.; Carlier, P. R.; Calter, M. A. & Ducker, W. A. (2002). Immobilized Enzymes as Catalytically-Active Tools for Nanofabrication. *Journal of the American Chemical Society*, Vol.124, No.41 (September 2002), pp. 12114-12115, ISSN 0002-7863.
- Kaholek, M.; Lee, W. K.; Ahn, S. J.; Ma, H.; Caster, K. C.; LaMattina, B. & Zauscher, S. (2004). Stimulus-Responsive Poly(N-isopropylacrylamide) Brushes and Nanopatterns Prepared by Surface-Initiated Polymerization. *Chemical of Materials*, Vol.16, No.19 (August 2004), pp. 3688-3696, ISSN 1520-5002.
- Sugimura, H. & Nakagiri, N. (1995). Degradation of a Trimethylsilyl Monolayer on Silicon Substrates Induced by Scanning Probe Anodization. *Langmuir*, Vol.11, No.10 (October 1995), pp. 3623-3625, ISSN 0743-7463.
- Amro, N. A.; Xu, S. & Liu, G. Y. (2000). Patterning Surfaces Using Tip-Directed Displacement and Self-Assembly. *Langmuir*, Vol.16, No.7 (March 2000), pp. 3006-3009, ISSN 0743-7463.
- Xu, S.; Miller, S.; Laibinis, P. E. & Liu, G. Y. (1999). Fabrication of Nanometer Scale Patterns within Self-Assembled Monolayers by Nanografting. *Langmuir*, Vol.15, No.21 (August 1999), pp. 7244-7251, ISSN 0743-7463.
- Liu, G. Y.; Xu, S. & Qian, Y. (2000). Nanofabrication of Self-Assembled Monolayers Using Scanning Probe Lithography. *Accounts of Chemical Research*, Vol.33, No.7 (March 2000), pp. 457-466, ISSN 1520-4898.
- Pena, D. J.; Raphael, M. P. & Byers, J. M. (2003). "Dip-Pen" Nanolithography in Registry with Photolithography for Biosensor Development. *Langmuir*, Vol.19, No.21 (September 2003), pp. 9028-9032, ISSN 0743-7463.
- Schwartz, P. V. (2002). Surface Functionalization and Stabilization of Mesoporous Silica Spheres by Silanization and Their Adsorption Characteristics. *Langmuir*, Vol.18, No.10 (April 2002), pp. 4014-4019, ISSN 0743-7463.
- Maynor, B. W.; Li, J.; Lu, C. & Liu, J. (2004). Site-Specific Fabrication of Nanoscale Heterostructures: Local Chemical Modification of GaN Nanowires Using Electrochemical Dip-Pen Nanolithography. *Journal of the American Chemical Society*, Vol.126, No.20 (May 2004), pp. 6409-6413, ISSN 0002-7863.
- Lee, SH.; Saito, N. & Takai, O. (2009). Highly reproducible technique for three-dimensional nanostructure fabrication via anodization scanning probe lithography. *Applied Surface Science*, Vol.255, No.16 (May 2009), PP. 7302-7306, ISSN 0169-4332.
- Lee, SH.; Ishizaki, T.; Saito, N. & Takai, O. (2007). Electrochemical soft lithography of an 1,7-octadiene monolayer covalently linked to hydrogen-terminated silicon using scanning probe Microscopy. *Surface Science*, Vol.601, No.18 (September 2007), pp. 4206-4211, ISSN 0039-6028.
- Lee, SH.; Ishizaki, T.; Saito, N. & Takai, O. (2007). Local generation of carboxyl groups on an organic monolayer through chemical conversion using scanning probe anodization.

Materials Science and Engineering C, Vol.27, No.5-8 (September 2007), pp. 1241-1246, ISSN 0928-4931.

Saito, N.; Lee, S.H.; Ishizaki, T.; Hieda, J.; Sugimura, H. & Takai, O. (2005). Surface-Potential Reversibility of an Amino-Terminated Self-Assembled Monolayer Based on Nanoprobe Chemistry. *The Journal of Physical Chemistry B*, Vol.109, No.23 (May 2005), pp. 11602-11605, ISSN 1089-5647.

Sugimura, H.; Saito, N.; Lee, S.H. & Takai, O. (2004). Reversible nanochemical conversion. *Journal of Vacuum Science & Technology B*, Vol.22, No.6 (November 2004), pp. L44-46, ISSN 1520-8567.

IntechOpen



Recent Advances in Nanofabrication Techniques and Applications

Edited by Prof. Bo Cui

ISBN 978-953-307-602-7

Hard cover, 614 pages

Publisher InTech

Published online 02, December, 2011

Published in print edition December, 2011

Nanotechnology has experienced a rapid growth in the past decade, largely owing to the rapid advances in nanofabrication techniques employed to fabricate nano-devices. Nanofabrication can be divided into two categories: "bottom up" approach using chemical synthesis or self assembly, and "top down" approach using nanolithography, thin film deposition and etching techniques. Both topics are covered, though with a focus on the second category. This book contains twenty nine chapters and aims to provide the fundamentals and recent advances of nanofabrication techniques, as well as its device applications. Most chapters focus on in-depth studies of a particular research field, and are thus targeted for researchers, though some chapters focus on the basics of lithographic techniques accessible for upper year undergraduate students. Divided into five parts, this book covers electron beam, focused ion beam, nanoimprint, deep and extreme UV, X-ray, scanning probe, interference, two-photon, and nanosphere lithography.

How to reference

In order to correctly reference this scholarly work, feel free to copy and paste the following:

SunHyung Lee, Takahiro Ishizaki, Katsuya Teshima, Nagahiro Saito and Osamu Takai (2011). Scanning Probe Lithography on Organic Monolayers, Recent Advances in Nanofabrication Techniques and Applications, Prof. Bo Cui (Ed.), ISBN: 978-953-307-602-7, InTech, Available from:

<http://www.intechopen.com/books/recent-advances-in-nanofabrication-techniques-and-applications/scanning-probe-lithography-on-organic-monolayers>

INTECH
open science | open minds

InTech Europe

University Campus STeP Ri
Slavka Krautzeka 83/A
51000 Rijeka, Croatia
Phone: +385 (51) 770 447
Fax: +385 (51) 686 166
www.intechopen.com

InTech China

Unit 405, Office Block, Hotel Equatorial Shanghai
No.65, Yan An Road (West), Shanghai, 200040, China
中国上海市延安西路65号上海国际贵都大饭店办公楼405单元
Phone: +86-21-62489820
Fax: +86-21-62489821

© 2011 The Author(s). Licensee IntechOpen. This is an open access article distributed under the terms of the [Creative Commons Attribution 3.0 License](#), which permits unrestricted use, distribution, and reproduction in any medium, provided the original work is properly cited.

IntechOpen

IntechOpen